

NACA RM E54F04



# RESEARCH MEMORANDUM

ACCELERATION OF HIGH-PRESSURE-RATIO SINGLE-SPOOL  
TURBOJET ENGINE AS DETERMINED FROM COMPONENT  
PERFORMANCE CHARACTERISTICS

III - EFFECT OF TURBINE STATOR ADJUSTMENT

By Harold E. Rohlik and John J. Rebeske

Lewis Flight Propulsion Laboratory  
CLASSIFICATION CHANGED Cleveland, Ohio

UNCLASSIFIED

LIBRARY COPY

AUG 4 1954

By authority of *NASA TPA 9* Date *9-1-59*

*713 11-20-59*

CLASSIFIED DOCUMENT

This material contains information affecting the national defense of the United States within the meaning of the espionage laws, Title 18, U.S.C., Sec. 793 and 794, the transmission or revelation of which in any manner to an unauthorized person is prohibited by law.

LANGLEY AERONAUTICAL LABORATORY  
LIBRARY, NACA  
LANGLEY FIELD, VIRGINIA

## NATIONAL ADVISORY COMMITTEE FOR AERONAUTICS

WASHINGTON

August 2, 1954

~~CONFIDENTIAL~~  
UNCLASSIFIED



## NATIONAL ADVISORY COMMITTEE FOR AERONAUTICS

RESEARCH MEMORANDUM

## ACCELERATION OF HIGH-PRESSURE-RATIO SINGLE-SPOOL TURBOJET ENGINE

## AS DETERMINED FROM COMPONENT PERFORMANCE CHARACTERISTICS

## III - EFFECT OF TURBINE STATOR ADJUSTMENT

By Harold E. Rohlik and John J. Rebeske, Jr.

## SUMMARY

An analytical investigation was made to determine from component performance the effect of turbine stator adjustment on the acceleration characteristics of a typical high-pressure-ratio single-spool turbojet engine. Turbine stator adjustment was adequate to permit engine operation in the intermediate-speed range, but was less satisfactory than the relatively simple schemes of compressor-interstage and -outlet bleed.

## INTRODUCTION

Studies of turbojet engine requirements for flight in the transonic range have revealed that a turbojet engine best suited for such flight would have a compressor pressure ratio of about 7 to 10 and a turbine-inlet temperature of about 2000° to 2300° R (ref. 1). However, when a single-spool axial-flow compressor is used in this pressure-ratio range, it may have poor off-design performance, particularly in the low-speed range (50 to 70 percent of design). In this low-speed range, the inlet stages operate in a low-efficiency high-angle-of-attack region and the outlet stages operate in a low-efficiency low-angle-of-attack region (ref. 2).

Equilibrium operation of an engine of this type with several exhaust-nozzle areas is described in reference 3. This reference shows that, in the intermediate-speed range (70 to 85 percent of design), all equilibrium operating lines of this particular engine enter the compressor surge region and the compressor will not accelerate through this region. Therefore, the component performance of the compressor and turbine, or the matching of these components, or both, must be altered to permit acceleration.

UNCLASSIFIED

Several means of improving the acceleration characteristics of such engines are compressor-outlet bleed, compressor-interstage bleed, adjustable compressor-inlet guide vanes and stator blades, and adjustable turbine stators. An investigation is being conducted at the NACA Lewis laboratory to evaluate the relative merits of such means for improving the acceleration characteristics of high-pressure-ratio single-spool turbojet engines.

Compressor-outlet bleed, compressor-interstage bleed, and combinations thereof are reported in references 4 and 5. Reference 4 shows that reasonable amounts of compressor-outlet bleed allowed high turbine-inlet temperatures during acceleration, and that the acceleration path should be as close to the surge region as is practical. Reference 5 reports that constant-area interstage bleed, properly located, gave smaller acceleration times than variable-area compressor-outlet bleed. Acceleration times achieved with variable-area compressor-outlet bleed and constant-area interstage bleed were 5.5 and 3.0 seconds, respectively, for surge-line operation. In the low-speed range of the fixed-geometry engine, turbine-inlet temperatures were limited to relatively low values by the flow-handling capacity of the turbine and the combination of relatively high weight flow and low turbine-inlet pressure provided by the compressor. In the intermediate-speed range, near the knee in the compressor surge line, the turbine-inlet temperature was limited to values which were too low to provide sufficient torque to drive the compressor. Adjusting the turbine stators to increase the throat areas permits larger equivalent weight flows and therefore higher inlet temperatures. This, in turn, increases the turbine torque if losses are not too large and improves the acceleration characteristics of the engine.

The purpose of this analysis is to evaluate turbine stator adjustment as a means of improving engine acceleration. Several combinations and degrees of stator adjustment are compared with respect to improved acceleration characteristics and mechanical simplicity.

## METHOD OF ANALYSIS

### Idealized Stator Adjustment

Determination of the potential improvement in acceleration characteristics of the engine under consideration by means of stator adjustment required a preliminary investigation. The effectiveness of turbine stator adjustment as a means of improving engine acceleration may be measured in terms of the time interval required to accelerate from idle to design speed. Therefore, in approaching the stator-adjustment problem, acceleration time and required flow increases were calculated for

an idealized stator-adjustment case that could be compared with previously established acceleration times obtained with compressor-interstage and -outlet bleed.

This idealized case was optimistic in that the specifications included surge-line operation of the compressor, constant turbine-inlet temperature of 2500° R (arbitrarily specified as the maximum allowable for short periods of time), and no bleed. For acceleration along the compressor surge line, reference 4 shows that, with design compressor and turbine geometry, the flow-handling capacity of the turbine necessitated compressor-outlet bleed in order to maintain a turbine-inlet temperature of 2500° R up to 88 percent of design speed. It was assumed, in this preliminary analysis, that the idealized stator adjustment permits the turbine to swallow the total compressor weight flow at a temperature of 2500° R up to a compressor speed of about 88 percent of design, at which speed design turbine geometry satisfies this condition and adjustment is no longer necessary. Turbine efficiencies were assumed to be the same as those for the similar acceleration in reference 4. An exhaust-nozzle area of 600 square inches, which was specified as the maximum allowable, was held constant in order to maximize turbine output. This acceleration path is indicated in figure 1 by the heavy line.

Measured component performance (figs. 1 to 3) with design geometry was used to calculate acceleration time for 2500° R operation. The mode of operation considered was the same as that for the variable-area compressor-outlet bleed case of reference 4, except that turbine torque at each speed was increased in direct proportion to the increase in turbine weight flow made possible by the idealized stator adjustment.

The time required for acceleration may be determined from the following equation:

$$\int_0^{\tau} d\tau = \int_{\omega_1}^{\omega_d} I \frac{d\omega}{\Gamma_t - (\Gamma_c + \Gamma_a)} = \frac{2\pi}{60} I \int_{N_1}^{N_d} \frac{dN}{\Delta\Gamma} = \frac{2\pi}{60} \frac{IN_d}{100} \int_{100 \frac{N_1}{N_d}}^{100} \frac{d \left( 100 \frac{N}{N_d} \right)}{\Delta\Gamma} \quad (1)$$

The graphical solution of equation (1) is presented in figure 4, which shows a total acceleration time of 3 seconds for the idealized case of stator adjustment. This acceleration time compares favorably with those of references 4 and 5. Figure 5 shows the increase in turbine-inlet equivalent weight flow necessary to achieve this acceleration time. This calculation shows an optimistic limit of improved

UNCLASSIFIED

engine acceleration that might be reached with stator adjustment and a range of turbine-inlet equivalent flow increases to be considered.

Although the idealized stator adjustment resulted in a satisfactory acceleration time, the actual weight-flow increases, turbine efficiencies, and hence acceleration times are functions of turbine geometry and internal flow conditions. Therefore, a more complete analysis was made taking these factors into consideration.

#### Acceleration Characteristics as Determined from Estimated Turbine Stage Performance

Turbine internal flow. - The changes in internal flow effected by turbine stator adjustment in a multistage turbine depend on the manner in which the stators are adjusted as well as the initial flow conditions. These changes are complex in nature because of the number of variables in the flow that are affected by stator adjustment. In obtaining an understanding of these changes, it is convenient to consider the general behavior of a turbine operating under conditions representative of those encountered in accelerating this particular engine. At the knee in the compressor surge line, at approximately 80 percent of compressor design speed, flow throughout the turbine and exhaust nozzle is subsonic, with pressure ratios of the three turbine stages approximately equal. With compressor operation fixed at this point, the turbine-inlet equivalent weight flow is increased by opening one or more rows of stator blades and increasing turbine-inlet temperature. With compressor operation, and hence mechanical speed, fixed, the increase in turbine torque associated with the increase in turbine-inlet temperature results in a greater acceleration rate at this speed. The turbine-outlet equivalent weight flow will increase at a somewhat slower rate than the inlet flow, and the turbine pressure ratio will decrease slightly. These variations are shown in figures 6 and 7, where changes in turbine-outlet equivalent flow and in turbine pressure ratio are plotted against turbine-inlet-flow change for this operation. The effect of turbine efficiency on these parameters is slight, one of the curves representing a constant turbine efficiency of 0.85 and the other a progressive decrease from an initial value of 0.85 to a value of 0.60 at an inlet equivalent flow increase of 42 percent. In these figures, the turbine pressure ratio is specified by the constant value of turbine-inlet total pressure and by the turbine-outlet total pressure required to satisfy continuity through the exhaust nozzle with atmospheric pressure at the exhaust-nozzle outlet.

The two methods of stator adjustment under consideration are the simultaneous adjustment of all three stages and the adjustment of the first-stage stator only. Each stage, in the case of three-stage

adjustment, operates with a nearly constant pressure ratio while both inlet and outlet equivalent weight flows increase. As the stators are opened, throat area is increased and turning is decreased. This results in a progressive unloading of the stator row with a decrease in the tangential component of velocity leaving the stator, and an increase in total pressure and hence Mach number relative to the rotor. As the stator loading decreases under these conditions, rotor flow conditions become more critical with relative velocities becoming sonic and then approaching the limiting loading condition. Stage efficiency necessarily changes during stator adjustment because of the changes in rotor incidence angles and stage outlet whirl. Whether the change is positive or negative at the outset depends, of course, upon the relation of the initial flow angles to the design angles. In either case, the efficiency decreases as the stator adjustment brings the rotor to limiting loading.

Adjustment of the first-stage stator only also results in an increase in flow-handling capacity of the turbine. As the first-stage stator flow area is increased to permit greater equivalent weight flows, the first-stage pressure ratio decreases somewhat, while the second- and third-stage pressure ratios increase. Since the second and third stages are not choked, this increase in second- and third-stage pressure ratio, coupled with the fact that equivalent speed decreases with an increase in temperature, means that these stages can now pass greater equivalent weight flows. As with three-stage adjustment, losses in each stage change because of the change in operating conditions of each stage. The direction and magnitude of the changes in losses and efficiency again depend upon the proximity of the initial operation to design operation, with an efficiency loss at extreme adjustments.

As the turbine stators are opened to increase flow capacity with the compressor operating point fixed, turbine torque increases with inlet temperature to the point at which further gains in temperature are offset by the increase in losses. Beyond this point, of course, turbine torque decreases.

Estimated turbine stage performance. - Performance of each of the three turbine stages was estimated with a simplified one-dimensional analysis for a range of speeds, pressure ratios, and stator adjustments. The ranges of turbine parameters considered in the analysis were speed, from 50 to 130 percent of design; pressure ratio, from 1.1 to about 1.9 in the first and second stages, and from 1.1 to limiting-loading in the third stage; and turbine stator adjustments, from design setting to 12° open. This method of performance estimation employed empirical loss coefficients obtained from detailed survey data from the original turbine operating at design speed and work. It was assumed that these coefficients were applicable over the complete ranges of operation and stator adjustment. Losses considered were limited to the viscous losses

in each blade row, which are associated with the level of internal flow velocities, rotor incidence-angle losses, and stage outlet whirl losses. Symbols and methods of estimating losses and other internal-flow phenomena are given in appendixes A and B, respectively.

Calculated stage performance was plotted in terms of inlet equivalent weight flow, equivalent torque, and temperature ratio. Examples of each are shown in figure 8, which represents third-stage performance with design stator setting.

Evaluation of stator adjustment. - Figure 4 shows that turbine torque available for acceleration, and therefore the rate of acceleration, is lowest at 50-percent design speed. This means that acceleration times for speed increments are largest in this range. However, figure 5 shows that 80-percent design speed is most critical in terms of turbine flow-handling capacity. At this speed, turbine stator adjustment must permit equivalent-flow increases up to 35 percent in order to utilize a turbine-inlet temperature of  $2500^{\circ}\text{R}$ . The 50- and 80-percent-speed points on the compressor surge line, then, were chosen as the operating points at which various degrees and combinations of stator adjustment were to be compared. At each compressor operating point, the actual weight flow, available pressure ratio, and mechanical speed were specified by the compressor operating characteristics. Turbine-inlet temperature, and thus turbine torque, was then determined by consideration of continuity through each turbine stage and the exhaust nozzle. In calculating the acceleration times, it was assumed that NACA standard sea-level conditions existed at the compressor inlet, and that transient component characteristics were the same as the steady-state conditions. In addition, the following assumptions were made:

Combustor total-pressure ratio, $p_3'/p_2'$ . . . . .	0.97
Stagnation pressure loss in tail pipe, lb/sq ft . . . . .	0
Fuel-air ratio, $w_f/w_c$ . . . . .	0.02
Leakage between compressor and turbine, $w_l/w_c$ . . . . .	0.02
Torque to drive accessories, $\Gamma_a$ , ft-lb . . . . .	3.0
Exhaust-nozzle area, $A_6$ , sq in. . . . .	600

The mode of operation was as follows: Acceleration began with the compressor operating at 50-percent design speed at surge, with the first or all three turbine stators open and the exhaust nozzle open to its maximum area of 600 square inches. Operation proceeded along the compressor surge line with turbine-inlet temperature varying continuously to satisfy continuity through the turbine and exhaust nozzle until the speed was attained at which the turbine-inlet temperature reached the maximum allowable value of  $2500^{\circ}\text{R}$ . Operation then followed the line

defined by this turbine geometry and a constant  $T_3'$  of 2500° R to a speed at which design turbine geometry permitted operation of the compressor at a pressure ratio below surge and at a  $T_3'$  of 2500° R. At this speed, the first or all three turbine stators were returned to their design position, and acceleration continued along the line specified by design geometry and  $T_3'$  of 2500° R to compressor design speed. These paths of operation are shown as the heavy lines in figure 9.

Results of these calculations, within the limits of accuracy of the stage-performance prediction method, provide a comparison between the adjustable-stator method and the methods of references 4 and 5 for improving the acceleration characteristics of this high-pressure-ratio single-spool turbojet engine.

## RESULTS AND DISCUSSION

### Increase in Flow-Handling Capacity

Figure 5 shows that the turbine stator adjustment most desirable with respect to engine acceleration should permit increases as great as 35 percent in equivalent weight flow with no loss in efficiency. The increase in turbine equivalent weight flow made possible by stator adjustment at a given speed depends upon the initial stator- and rotor-throat Mach numbers, the stator-outlet angle (which determines the rate of change of area with adjustment), and the change in internal loss as the stators are opened. The initial turbine operating condition as well as the initial turbine geometry, then, determine the potentialities of turbine stator adjustment for any given situation. The magnitudes of turbine-inlet equivalent flow increases possible for a range of engine operating conditions, including fixed compressor operation, are presented in reference 6, in which operation is considered wherein one or more blade rows are choked.

The increases in stator-throat area calculated for the stator adjustment of 12° were 42 percent in the first stage, 31 percent in the second stage, and 24 percent in the third stage. Estimated performance shows that increases in the equivalent weight flow were in every case considerably smaller than those in the stator-throat area. The effect of stator adjustment on equivalent weight flow in the first stage is presented in figure 10 for three equivalent speeds and a constant stage pressure ratio of 1.5. An increase in stator-throat area of 40 percent at 90 percent of design equivalent speed results in a gain of only 20 percent in equivalent weight flow. Limitations imposed by the rotor-throat area and internal losses keep the flow increase to a relatively low value.



### Comparison of Stator-Adjustment Combinations

Idle speed and the knee in the surge line present the greatest problems in surge-line operation through the low- and intermediate-speed range. Idle speed is critical in that the torque available for acceleration and, hence, the acceleration rates are smallest here, even in the idealized case; while, at the knee in the compressor surge line, matching characteristics of the unmodified engine are such that the turbine-inlet temperature is limited to values too low to provide sufficient torque for driving the compressor.

In order to evaluate stator adjustment in the range of adjustment considered, compressor operation at these points was specified, and turbine torque was calculated for the following five combinations of stator adjustment:

Combination	First-stage adjustment, deg	Second-stage adjustment, deg	Third-stage adjustment, deg
1 (design)	0	0	0
2	6	6	6
3	12	12	12
4	6	0	0
5	12	0	0

Calculations were made for an exhaust-nozzle area of 600 square inches. Figure 11 shows turbine-inlet equivalent weight flow, turbine pressure ratio, turbine efficiency, and turbine equivalent speed plotted against stator adjustment for the two methods of adjustment at 80-percent compressor design speed. The dashed portions are extrapolated.

In order to estimate the trends of the torque curves at stator adjustments larger than those calculated, extrapolated values from figure 11 were used to calculate turbine torque values in the adjustment range beyond 12°. Figure 12 shows the variation of turbine torque with stator adjustment. The dashed portions represent values calculated from the extrapolated values of figure 11. For three-stage adjustment, the maximum value of equivalent turbine torque, about 3530 foot-pounds, occurs at a stator adjustment of approximately 10°. The first-stage adjustment at which torque is maximized is approximately 14°, and the peak value is about 3400 foot-pounds. At 80 percent of compressor design speed, the torque required to drive the compressor is 3117 foot-pounds. Therefore, although the turbine torque resulting from three-stage adjustment is only 4 percent greater than that obtained with first-stage adjustment, the net difference available for acceleration is about 46 percent greater.

3230 The variations of turbine-inlet equivalent weight flow, turbine pressure ratio, turbine efficiency, and turbine equivalent speed with stator adjustment at 50-percent or idle speed are shown in figure 13. The dashed portions are extrapolated. Figure 14 presents the corresponding variation in turbine torque, the dashed portions representing values calculated from extrapolated values of figure 13. At idle speed, three-stage adjustment provides the maximum torque, about 2300 foot-pounds, at a setting of  $12^\circ$ . First-stage stator adjustment is slightly less effective, reaching a peak torque value of 2200 foot-pounds at a stator adjustment of about  $14^\circ$ . The torque obtained with three-stage adjustment is slightly larger (5 percent) than that obtained with first-stage adjustment. Required compressor torque at idle speed is 1930 foot-pounds, however, which means that three-stage adjustment provided 37 percent more torque for acceleration.

#### Acceleration Time

CE-2 Acceleration times were calculated for combinations 3 and 5. Combination 5 (first stator opened  $12^\circ$ ) was selected because of the greater desirability of single-stage adjustment, and combination 3 (all stators opened  $12^\circ$ ) because it provided maximum or very nearly maximum torque at the two speeds considered. The graphical integration for acceleration time (9.6 sec) with combination 5 is shown in figure 15(a), and that with combination 3 (7.0 sec) is shown in figure 15(b). Although these times are unrealistic, inasmuch as surge-line operation is unrealistic, they provide a basis for comparison among the various methods considered for improving acceleration characteristics. These acceleration times of 9.6 and 7.0 seconds are considerably greater than the 3.0 seconds obtained with the idealized calculation, because large gains in turbine-inlet equivalent flow were not obtained at high efficiencies. Consequently, for the methods of stator adjustment selected, turbine-inlet temperature was limited to relatively low values through most of the speed range. The calculated values of  $T_3$  are plotted against percent of compressor design speed in figure 16.

The acceleration times calculated for surge-line operation with adjustable turbine stators are compared in figure 17 with acceleration times calculated for surge-line operation with outlet bleed and interstage bleed, which were reported in references 4 and 5. This figure shows that acceleration times as low as 3.0 seconds were obtained with the relatively simple constant-area interstage bleed at the outlet of the 12<sup>th</sup> compressor stage. Reference 5 also presents acceleration times calculated for operation at pressure ratios below surge with the same interstage bleed. Operation along a line at 96 percent of surge pressure ratio resulted in an acceleration time of about 4.3 seconds. Acceleration times for operation at pressure ratios below surge would be greater than 9.6 seconds with first-stage stator adjustment, and greater than 7.0 seconds with three-stage adjustment.

## SUMMARY OF RESULTS

From an analytical investigation made to determine the effect of turbine stator adjustment on the acceleration characteristics of a typical high-pressure-ratio single-spool turbojet engine, the following results were obtained:

1. Estimated turbine performance showed that acceleration of the engine through the low- and intermediate-speed range can be achieved with adjustable turbine stators.

2. Among the cases considered at the knee in the compressor surge line at about 80 percent of design speed, maximum torque obtainable with three-stage turbine stator adjustment was approximately 4 percent greater than the maximum obtainable with first-stage stator adjustment only. The increment of torque in excess of compressor torque and therefore available for acceleration was approximately 46 percent greater. At idle speed, three-stage stator adjustment provided a maximum torque 5 percent greater than the maximum obtainable with first-stage adjustment only. The torque available for acceleration was about 37 percent greater.

3. Acceleration times of 9.6 and 7.0 seconds were calculated for first-stage and three-stage stator settings of  $12^\circ$  from the design setting through the low- and intermediate-speed range and surge-line compressor operation. A time of 3.0 seconds was obtained for constant-area compressor-interstage bleed.

4. For all cases considered, increases in equivalent weight flow were smaller than the corresponding increases in stator-throat area, particularly in the high-speed range and for the larger stator adjustments.

## CONCLUSION

Stator adjustment in the three-stage turbine of the high-pressure-ratio single-spool turbojet engine under consideration was investigated as a means of improving acceleration characteristics. Results of this investigation showed that turbine stator adjustment is less effective in terms of time required to accelerate to design speed than the relatively simple schemes of compressor-outlet and -interstage air bleed. Therefore, adjustable turbine stators alone are not a satisfactory solution to the problem.

Lewis Flight Propulsion Laboratory  
National Advisory Committee for Aeronautics  
Cleveland, Ohio, June 7, 1954

## APPENDIX A

## SYMBOLS

The following symbols are used in this report:

A	flow area, sq ft
$a_{cr}$	critical velocity, $\sqrt{2\gamma gRT/\gamma + 1}$ , ft/sec
C	constant ratio of outlet tangential velocity to throat velocity, $\sqrt{1 - \left(\frac{O + e}{S}\right)^2}$
$c_p$	specific heat at constant pressure, Btu/(lb)(°R)
$c_v$	specific heat at constant volume, Btu/(lb)(°R)
e	blade trailing-edge thickness, in.
g	acceleration due to gravity, 32.17 ft/sec <sup>2</sup>
I	polar moment of inertia, (ft-lb)(sec <sup>2</sup> )
J	mechanical equivalent of energy, ft-lb/Btu
K	local loss coefficient
N	rotational speed, rpm
O	throat opening, in.
p	pressure, lb/sq ft
R	gas constant, ft-lb/(lb)(°R)
S	blade pitch, in.
T	temperature, °R
U	wheel speed, ft/sec
V	velocity, ft/sec
W	velocity relative to rotor, ft/sec

3230

CE-2 back

w weight flow, lb/sec  
 $\beta$  blade inlet mean camber angle, deg  
 $\Gamma$  torque, ft-lb  
 $\Delta\Gamma$  torque available for acceleration,  $\Gamma_t - (\Gamma_c + \Gamma_a)$ , ft-lb  
 $\gamma$  ratio of specific heats,  $c_p/c_v$   
 $\delta$  stagnation pressure ratio,  $p'/p_0$   
 $\eta$  adiabatic efficiency  
 $\theta$  stagnation temperature ratio,  $T'/T_0$   
 $\rho$  gas density, lb/cu ft  
 $\tau$  time, sec  
 $\nu$  deviation angle, deg from blade inlet mean camber angle  
 $\omega$  angular velocity, radians/sec

## Subscripts:

a accessories  
c compressor  
d design  
f fuel  
i idle  
l leakage  
r rotor  
ro rotor outlet  
rt rotor throat  
s stator

3230

si stator inlet  
so stator outlet, rotor inlet  
st stator throat  
t turbine  
u tangential component  
x axial component  
0 NACA standard sea-level conditions  
1 compressor inlet  
2 compressor outlet  
3 turbine inlet  
4 second turbine stage inlet  
5 third turbine stage inlet  
6 exhaust nozzle

## Superscripts:

' stagnation condition  
" stagnation condition relative to rotor

## APPENDIX B

## STAGE-PERFORMANCE ESTIMATION PROCEDURE

The procedure employed to estimate turbine stage performance was a simplified one-dimensional analysis in which it was assumed that the internal losses were as follows:

1. Viscous losses associated with blade profile and wall drag, which could be expressed as a function of the local critical-velocity ratio and an empirical loss coefficient that was constant for all operation
2. Rotor incidence losses, which consisted of the total of the kinetic energy associated with the inlet velocity component normal to the blade inlet camber angle
3. Stage-outlet whirl losses, which in the first and second stages consisted of the total of the kinetic energy associated with the component of the stage-outlet velocity normal to the inlet camber angle of the stator blades of the second and third stages, respectively, and which in the third stage consisted of the kinetic energy of the tangential component of stage-outlet velocity.

Stage calculations were made for NACA standard conditions at the inlet. The procedure is briefly described in the following steps, which were typical of all subsonic operation. Operation with one or both blade rows choked, which was treated in a slightly different manner, is also described.

## No Choking

Step 1. - Stator-throat critical-velocity ratio is specified, and weight flow is calculated as follows:

$$w = A_{st} p_{si} \sqrt{\frac{2\gamma g}{(\gamma+1)RT_{si}}} \left(\frac{V}{a_{cr}}\right)_{st} \left[1 - K_{st} \left(\frac{V}{a_{cr}}\right)_{st}^2\right] \left[1 - \frac{\gamma-1}{\gamma+1} \left(\frac{V}{a_{cr}}\right)_{st}^2\right]^{\frac{1}{\gamma-1}} \quad (1)$$

where  $K_{st}$  is the stator-throat local loss coefficient. The nozzle-outlet tangential critical-velocity ratio is

$$\left(\frac{V_u}{a_{cr}'}\right)_{so} = \left(\frac{V}{a_{cr}'}\right)_{st} \times C_s \quad (2)$$

where  $C_s$  is a constant determined from stator geometry.

Step 2. - Stator-outlet critical-velocity ratio is obtained by iteration, and by assuming first a value of stator-outlet critical-velocity ratio and then checking this with the flow charts of reference 7, the known  $(V_u/a_{cr}')_{so}$ , and the approximate value of

$$\left(\frac{\rho V_x}{\rho' a_{cr}'}\right)_{so} = \frac{w}{A_{so} p_{s1}'} \frac{1}{\left[1 - K_{so} \left(\frac{V}{a_{cr}'}\right)_{so}^2\right] \sqrt{\frac{2\gamma g}{(\gamma+1)RT_{s1}'}}} \quad (3)$$

based on the assumed  $(V/a_{cr}')_{so}$ . When the assumed value of  $(V/a_{cr}')_{so}$  and the value read from the chart agree, stator-outlet conditions are known.

Step 3. - With a specified wheel speed  $(U/a_{cr}')_{so}$ , relative total temperature is calculated:

$$\left(\frac{T''}{T'}\right)_{so} = 1 - \frac{\gamma-1}{\gamma+1} \left[ 2 \left(\frac{V_u}{a_{cr}'}\right)_{so} \left(\frac{U}{a_{cr}'}\right)_{so} - \left(\frac{U}{a_{cr}'}\right)_{so}^2 \right] \quad (4)$$

Step 4. - Static pressure and temperature at the stator outlet are calculated by the following equations:

$$\left(\frac{T}{T'}\right)_{so} = 1 - \frac{\gamma-1}{\gamma+1} \left(\frac{V}{a_{cr}'}\right)_{so}^2 \quad (5)$$

$$p_{so} = p_{s1}' \left[ 1 - K_{so} \left(\frac{V}{a_{cr}'}\right)_{so}^2 \right] \left[ 1 - \frac{\gamma-1}{\gamma+1} \left(\frac{V}{a_{cr}'}\right)_{so}^2 \right]^{\frac{\gamma}{\gamma-1}} \quad (6)$$

Step 5. - Rotor-inlet deviation angle is calculated by

$$\nu_r = \beta_r - \tan^{-1} \left( \frac{\frac{V_u}{a_{cr}'} - \frac{U}{a_{cr}'}}{\frac{V_x}{a_{cr}'}} \right)_{so} \quad (7)$$



and critical-velocity ratio by

$$\left(\frac{W}{a_{cr}^*}\right)_{so} = \sqrt{\left(\frac{V_x}{a_{cr}^*}\right)_{so}^2 + \left[\left(\frac{V_u}{a_{cr}^*}\right)_{so} - \left(\frac{U}{a_{cr}^*}\right)_{so}\right]^2} \quad (8)$$

Step 6. - Rotor-inlet relative total pressure  $p_{so}''$  is calculated with the following equation:

$$\left(\frac{p''}{p}\right)_{so} = \left[\left(\frac{T''}{T}\right)_{so} - \frac{\gamma-1}{\gamma+1} \left(\frac{T'}{T}\right)_{so} (\sin^2 \alpha_r) \left(\frac{W}{a_{cr}^*}\right)_{so}^2\right]^{\frac{\gamma}{\gamma-1}} \quad (9)$$

Step 7. - Rotor-throat critical-velocity ratio is obtained with the following equation:

$$w = A_{rt} p_{so}'' \sqrt{\frac{2\gamma g}{(\gamma+1)RT''}} \left(\frac{W}{a_{cr}''}\right)_{rt} \left[1 - K_{rt} \left(\frac{W}{a_{cr}''}\right)_{rt}^2\right] \left[1 - \frac{\gamma-1}{\gamma+1} \left(\frac{W}{a_{cr}''}\right)_{rt}^2\right]^{\frac{1}{\gamma-1}} \quad (10)$$

Step 8. - Rotor-outlet tangential critical-velocity ratio is calculated by

$$\left(\frac{W_u}{a_{cr}''}\right)_{ro} = \left(\frac{W}{a_{cr}''}\right)_{rt} \times C_r \quad (11)$$

and outlet flow parameter by

$$\left(\frac{\rho W_x}{\rho'' a_{cr}''}\right)_{ro} = \frac{w}{A_{ro} p_{so}''} \frac{1}{\left[1 - K_{ro} \left(\frac{W}{a_{cr}''}\right)_{ro}^2\right] \sqrt{\frac{2\gamma g}{(\gamma+1)RT''}}} \quad (12)$$

in the same manner as in step 2.

Step 9. - Rotor-outlet total temperature is obtained from

$$\left(\frac{T'}{T''}\right)_{ro} = 1 - \frac{\gamma-1}{\gamma+1} \left[2 \left(\frac{W_u}{a_{cr}''}\right)_{ro} \left(\frac{U}{a_{cr}''}\right)_{ro} - \left(\frac{U}{a_{cr}''}\right)_{ro}^2\right] \quad (13)$$

Step 10. - Static temperature and pressure at rotor outlet are calculated:

$$\left(\frac{T}{T''}\right)_{ro} = 1 - \frac{\gamma-1}{\gamma+1} \left(\frac{W}{a_{cr}}\right)_{ro}^2 \quad (14)$$

and

$$p_{ro} = p''_{so} \left[ 1 - K_{ro} \left(\frac{W}{a_{cr}}\right)_{ro}^2 \right] \left[ 1 - \frac{\gamma-1}{\gamma+1} \left(\frac{W}{a_{cr}}\right)_{ro}^2 \right]^{\frac{\gamma}{\gamma-1}} \quad (15)$$

Step 11. - Deviation angle at rotor outlet is calculated:

$$\nu_{ro} = \beta_s - \tan^{-1} \left( \frac{\frac{W_u}{a_{cr}} - \frac{U}{a_{cr}}}{\frac{W_x}{a_{cr}}} \right)_{ro} \quad (16)$$

where  $\beta_s$  is the inlet angle of the subsequent stator in first- and second-stage calculations, and is zero in the third-stage calculations.

Step 12. - With rotor-outlet conditions known,

$$\left(\frac{V}{a_{cr}}\right)_{ro} = \sqrt{\left(\frac{W_x}{a_{cr}}\right)_{ro}^2 + \left[\left(\frac{W_u}{a_{cr}}\right)_{ro} - \left(\frac{U}{a_{cr}}\right)_{ro}\right]^2} \quad (17)$$

stage-outlet total pressure is calculated:

$$\left(\frac{p'}{p}\right)_{ro} = \left[\left(\frac{T'}{T}\right)_{ro} - \frac{\gamma-1}{\gamma+1} \left(\frac{T''}{T}\right)_{ro} (\sin^2 \nu_{ro}) \left(\frac{V}{a_{cr}}\right)_{ro}^2\right]^{\frac{\gamma}{\gamma-1}} \quad (18)$$

Step 13. - Stage torque is calculated:

$$\Gamma = \frac{60Jwc_p(T'_{s1} - T'_{ro})}{2\pi N} \quad (19)$$

Stage pressure ratio, speed, weight flow, torque and stage temperature ratio are now known. Since NACA standard sea-level conditions were assumed at the inlet, the values obtained are equivalent values.

### Stator Choking

When the stator is choked and stator-outlet velocities are supersonic, values of  $(V/a'_{cr})_{so}$  of 1.0 and greater are specified and the weight flow  $w$  is the value corresponding to  $(V/a'_{cr})_{st} = 1.0$ . Stator-outlet axial critical-velocity ratio is obtained from

$$\left(\frac{V_x}{a'_{cr}}\right)_{so} = \frac{w \sqrt{\frac{(\gamma+1)RT'_{s1}}{2\gamma g}}}{p'_{s1} A_{so} \left[1 - K_{so} \left(\frac{V}{a'_{cr}}\right)_{so}^2\right] \left[1 - \frac{\gamma-1}{\gamma+1} \left(\frac{V}{a'_{cr}}\right)_{so}^2\right]^{\frac{1}{\gamma-1}}} \quad (20)$$

and

$$\left(\frac{V_u}{a'_{cr}}\right)_{so} = \sqrt{\left(\frac{V}{a'_{cr}}\right)_{so}^2 - \left(\frac{V_x}{a'_{cr}}\right)_{so}^2} \quad (21)$$

With these quantities known, rotor-inlet conditions can be calculated as in step 3 and calculation can proceed as before.

### Rotor Choking

With  $(W/a''_{cr})_{rt} = 1.0$ , the value of

$$\left(\frac{W}{a''_{cr}}\right)_{rt} \left[1 - \frac{\gamma-1}{\gamma+1} \left(\frac{W}{a''_{cr}}\right)_{rt}^2\right]^{\frac{1}{\gamma-1}} \left[1 - K_{rt} \left(\frac{W}{a''_{cr}}\right)_{rt}^2\right]$$

is determined. This corresponds to the correct value of

$$\frac{w}{A_{rt} p_{so}} \sqrt{\frac{(\gamma+1)RT''}{2\gamma g}}$$

which is uniquely specified for each value of  $(V/a'_{cr})_{so}$  if the stator is choked, or  $(V/a'_{cr})_{st}$  if the stator is not choked. A simple plot of  $\frac{w}{A_{rt} p_{so}''} \sqrt{\frac{(\gamma+1)RT''}{2\gamma g}}$  as a function of  $\left(\frac{V}{a'_{cr}}\right)_{so}$  or  $\left(\frac{V}{a'_{cr}}\right)_{st}$  gives the value of  $(V/a'_{cr})_{so}$  that corresponds to  $(W/a''_{cr})_{rt} = 1.0$ , and with this value calculations may be repeated from step 1 if the stator is not choked, or by the supersonic stator-outlet calculation if the stator is choked.

With  $w$  corresponding to  $(W/a''_{cr})_{rt} = 1.0$ , a solution for  $(W_x/a''_{cr})_{ro}$  is obtained with assumed values of  $(W/a''_{cr})_{ro}$  of 1.0 and greater:

$$\left(\frac{W_x}{a''_{cr}}\right)_{so} = \frac{w \sqrt{\frac{(\gamma+1)RT''}{2\gamma g}}}{p_{so}'' \left[1 - K_{ro} \left(\frac{W}{a''_{cr}}\right)_{ro}^2\right] \left[1 - \frac{\gamma-1}{\gamma+1} \left(\frac{W}{a''_{cr}}\right)_{ro}^2\right]^{\frac{1}{\gamma-1}}} \quad (22)$$

Then,

$$\left(\frac{W_u}{a''_{cr}}\right)_{ro} = \sqrt{\left(\frac{W}{a''_{cr}}\right)_{ro}^2 - \left(\frac{W_x}{a''_{cr}}\right)_{ro}^2} \quad (23)$$

With rotor-outlet critical-velocity ratios known, stage-outlet conditions and torque may be calculated as in steps 9 to 12.

#### REFERENCES

1. Lubarsky, Bernard: Performance and Load-Range Characteristics of Turbojet Engine in Transonic Speed Range. NACA TN 2088, 1950.
2. Medeiros, Arthur A., Benser, William A., and Hatch, James E.: Analysis of Off-Design Performance of a 16-Stage Axial-Flow Compressor with Various Blade Modifications. NACA RM E52L03, 1953.
3. Rebeske, John J., Jr., and Dugan, James F., Jr.: Matched Performance Characteristics of a 16-Stage Axial-Flow Compressor and a 3-Stage Turbine. NACA RM E52H18, 1953.

4. Rebeske, John J., Jr., and Rohlik, Harold E.: Acceleration of High-Pressure-Ratio Single-Spool Turbojet Engine as Determined from Component Performance Characteristics. I - Effect of Air Bleed at Compressor Outlet. NACA RM E53A09, 1953.
5. Rebeske, John J., Jr., and Dugan, James F., Jr.: Acceleration of High-Pressure-Ratio Single-Spool Turbojet Engine as Determined from Component Performance Characteristics. II - Effect of Compressor Interstage Air Bleed. NACA RM E53E06, 1953.
6. English, Robert E., and Cavicchi, Richard H.: One-Dimensional Analysis of Choked-Flow Turbines. NACA Rep. 1127, 1953. (Supersedes NACA TN 2810.)
7. Alpert, Sumner, and Litrenta, Rose M.: Construction and Use of Charts in Design Studies of Gas Turbines. NACA TN 2402, 1951.

3230

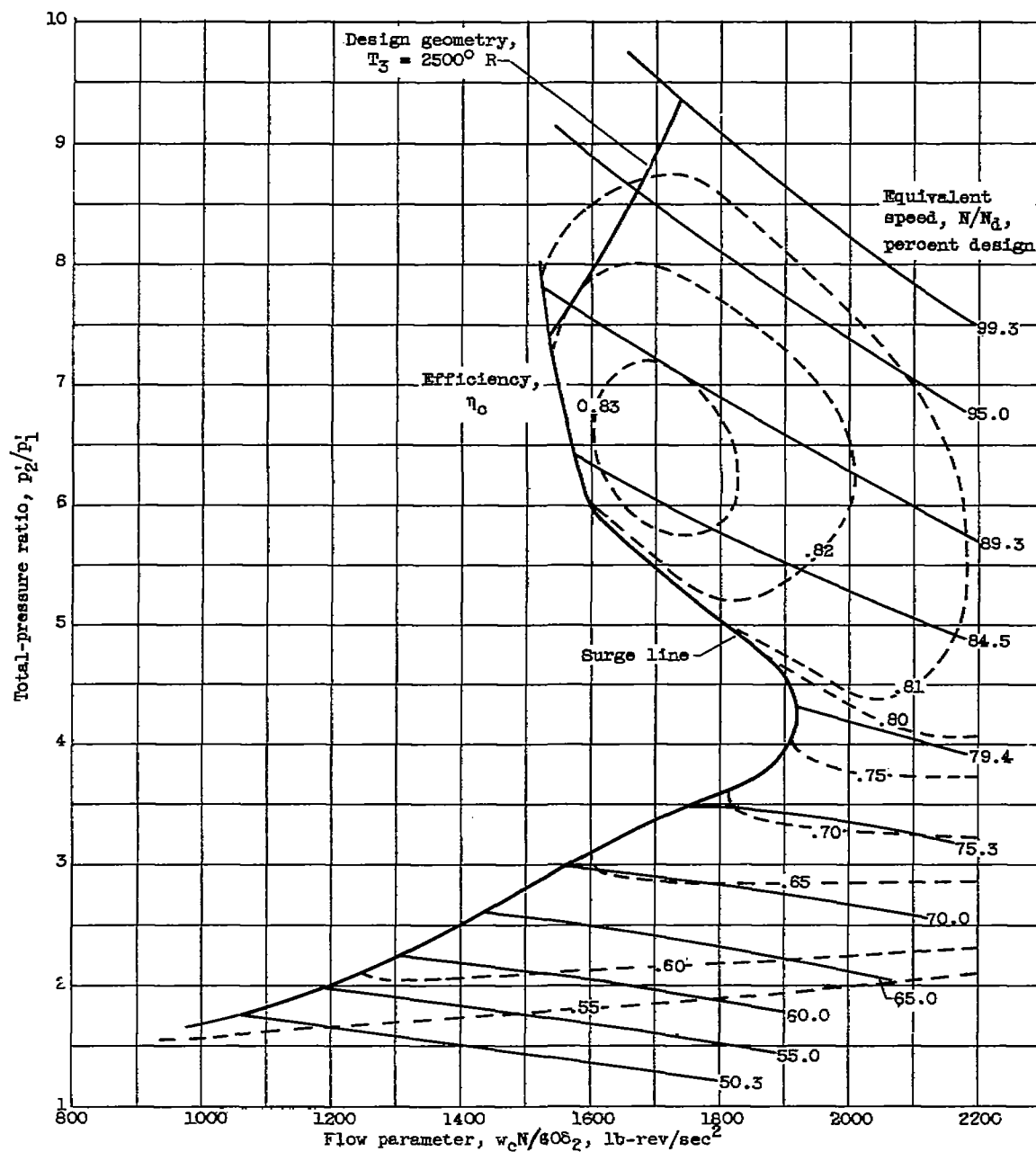


Figure 1. - Compressor performance map.

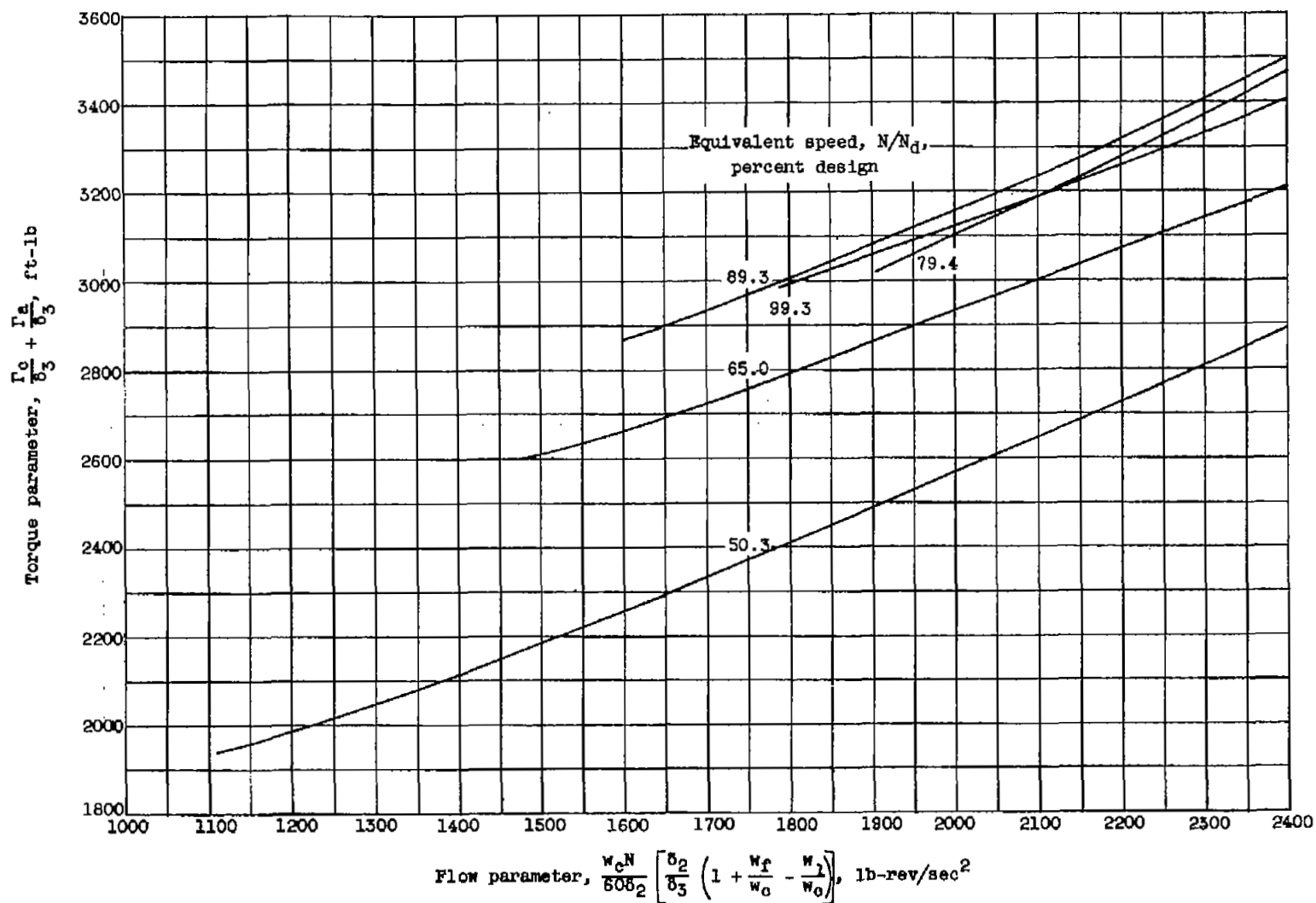


Figure 2. - Compressor torque characteristics.

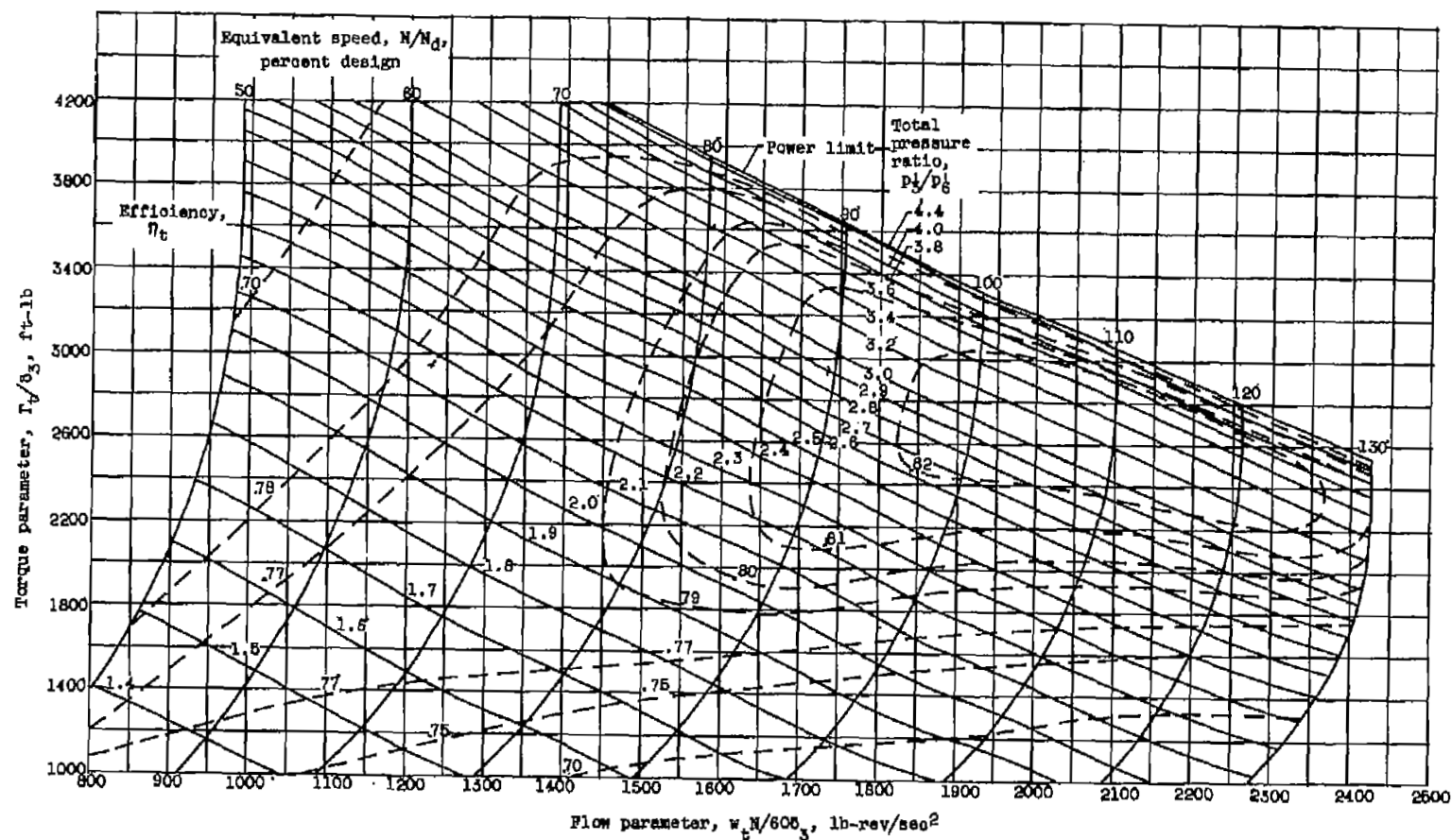


Figure 3. -- Turbine performance map.



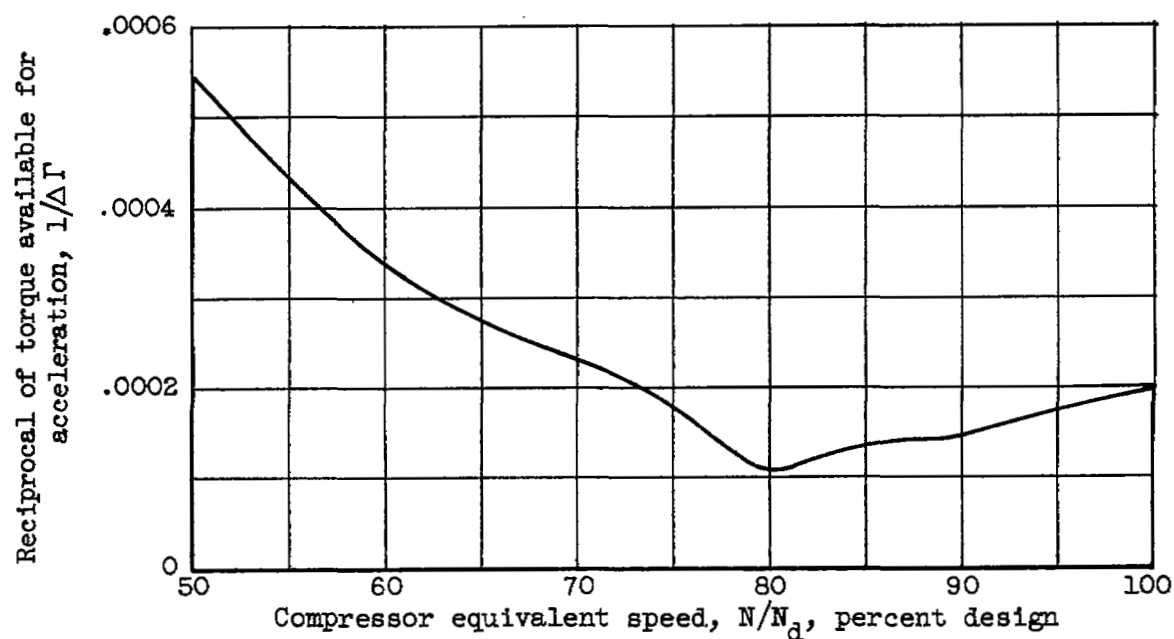


Figure 4. - Graphical integration for acceleration time. Total acceleration time, 3 seconds; turbine-inlet temperature,  $2500^{\circ}\text{R}$ ; surge pressure ratio; compressor weight flow equal to turbine weight flow.

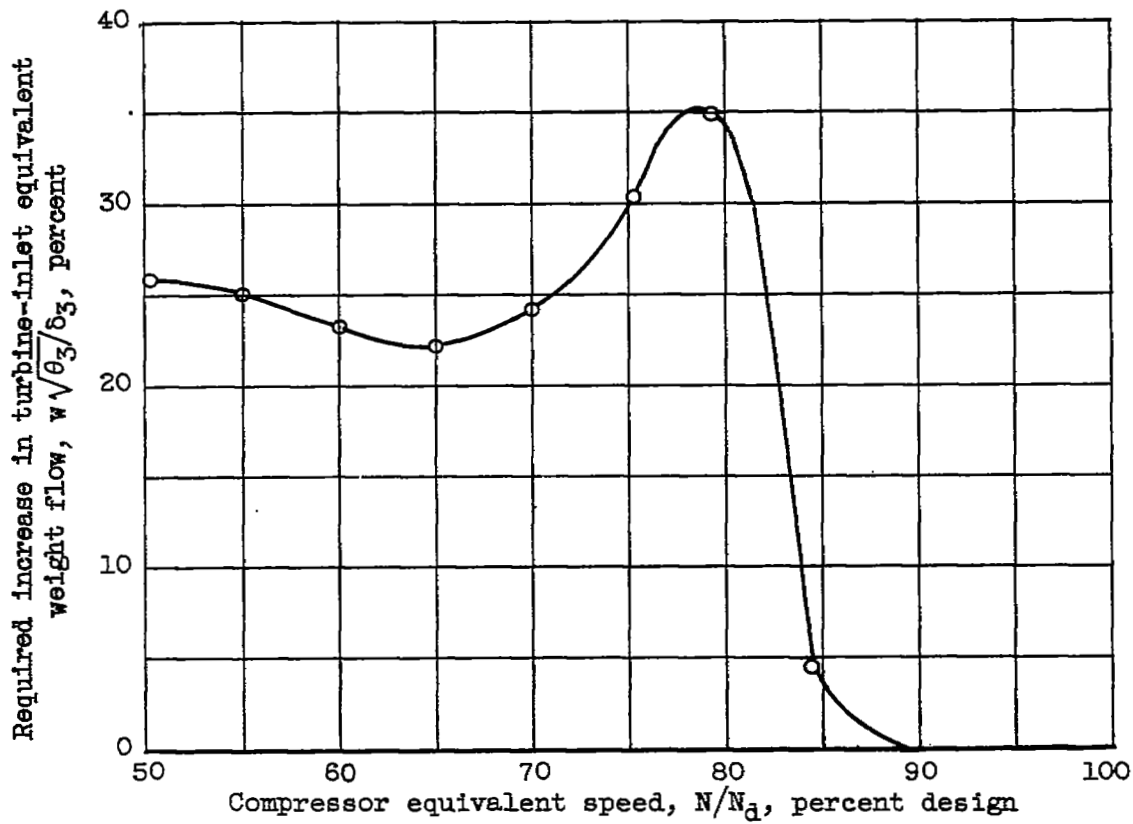


Figure 5. - Increase in turbine-inlet equivalent weight flow required for conditions of figure 4.

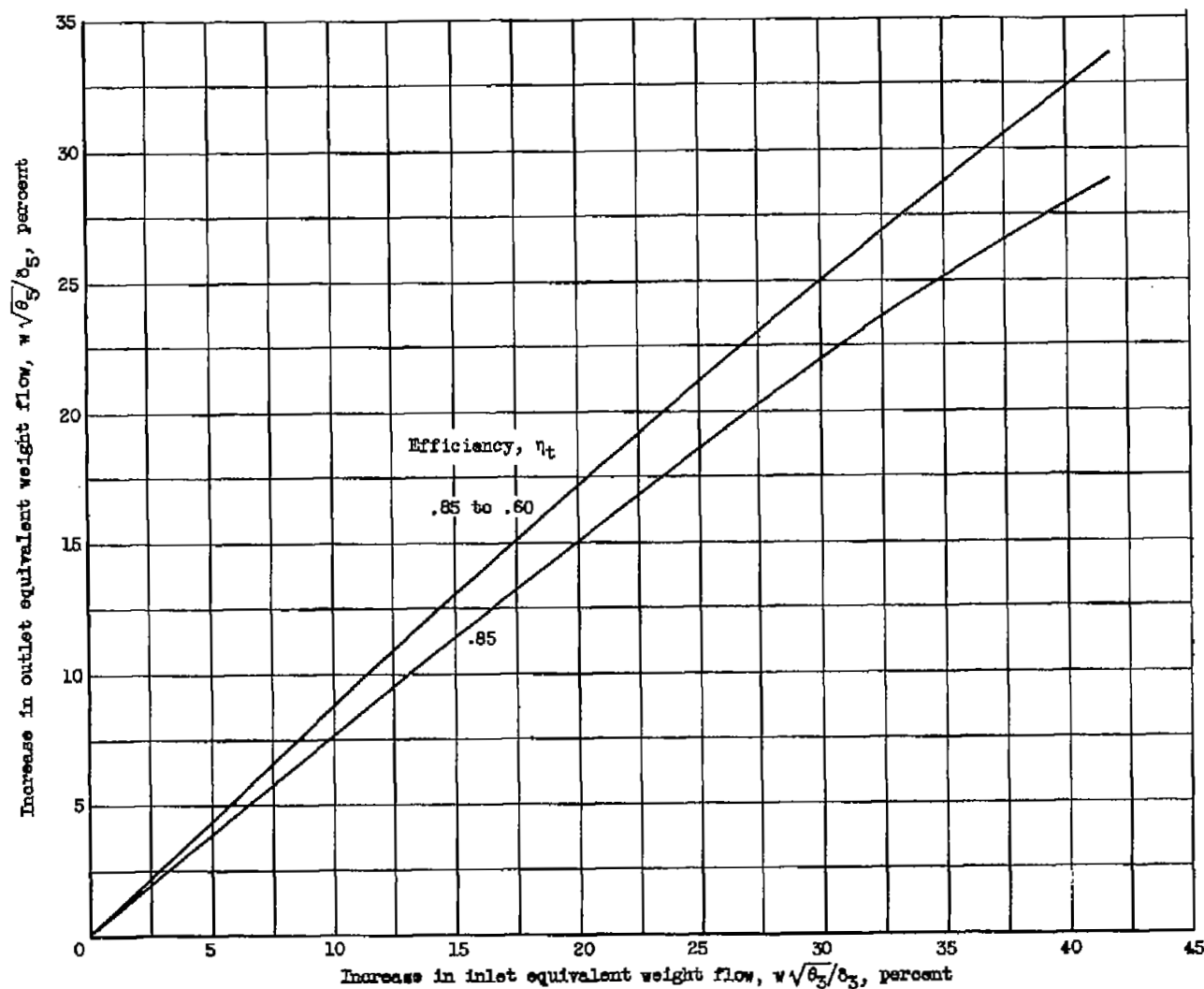


Figure 6. - Variation of percentage increase in turbine-outlet equivalent flow with percentage increase in turbine-inlet equivalent flow for compressor operation fixed at knee in surge line. Exhaust-nozzle area, 600 square inches.

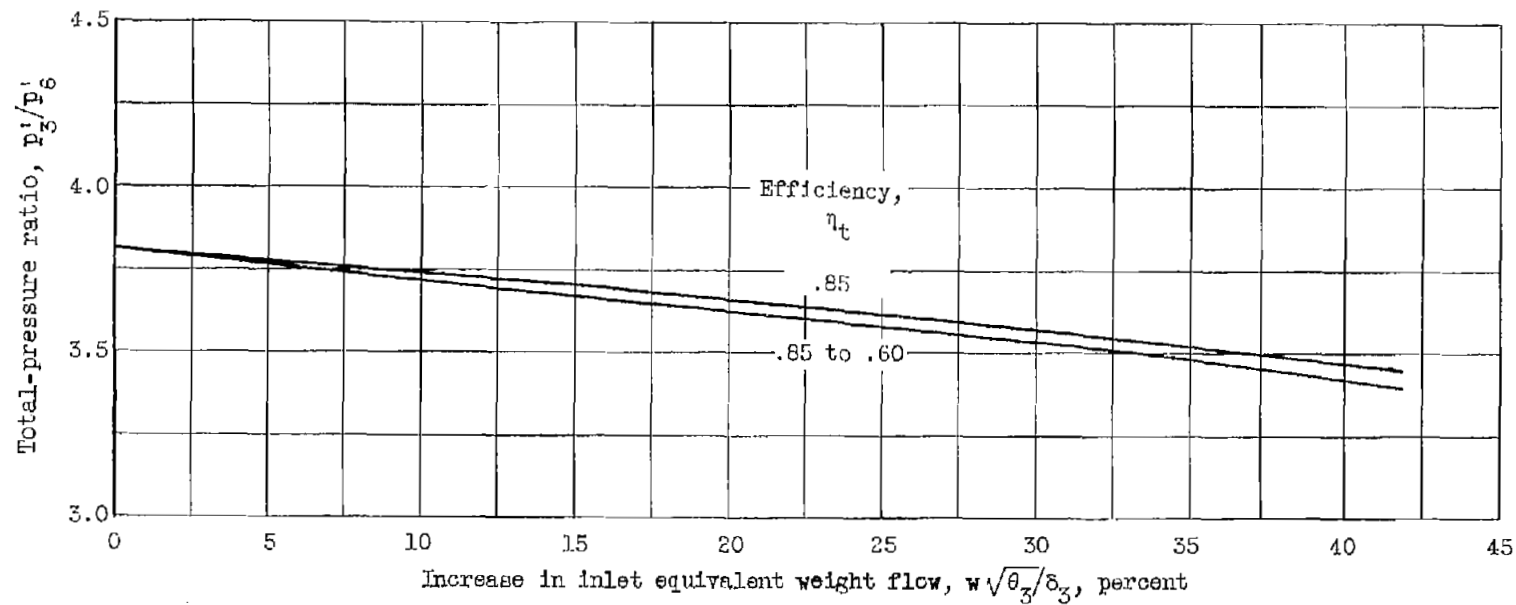
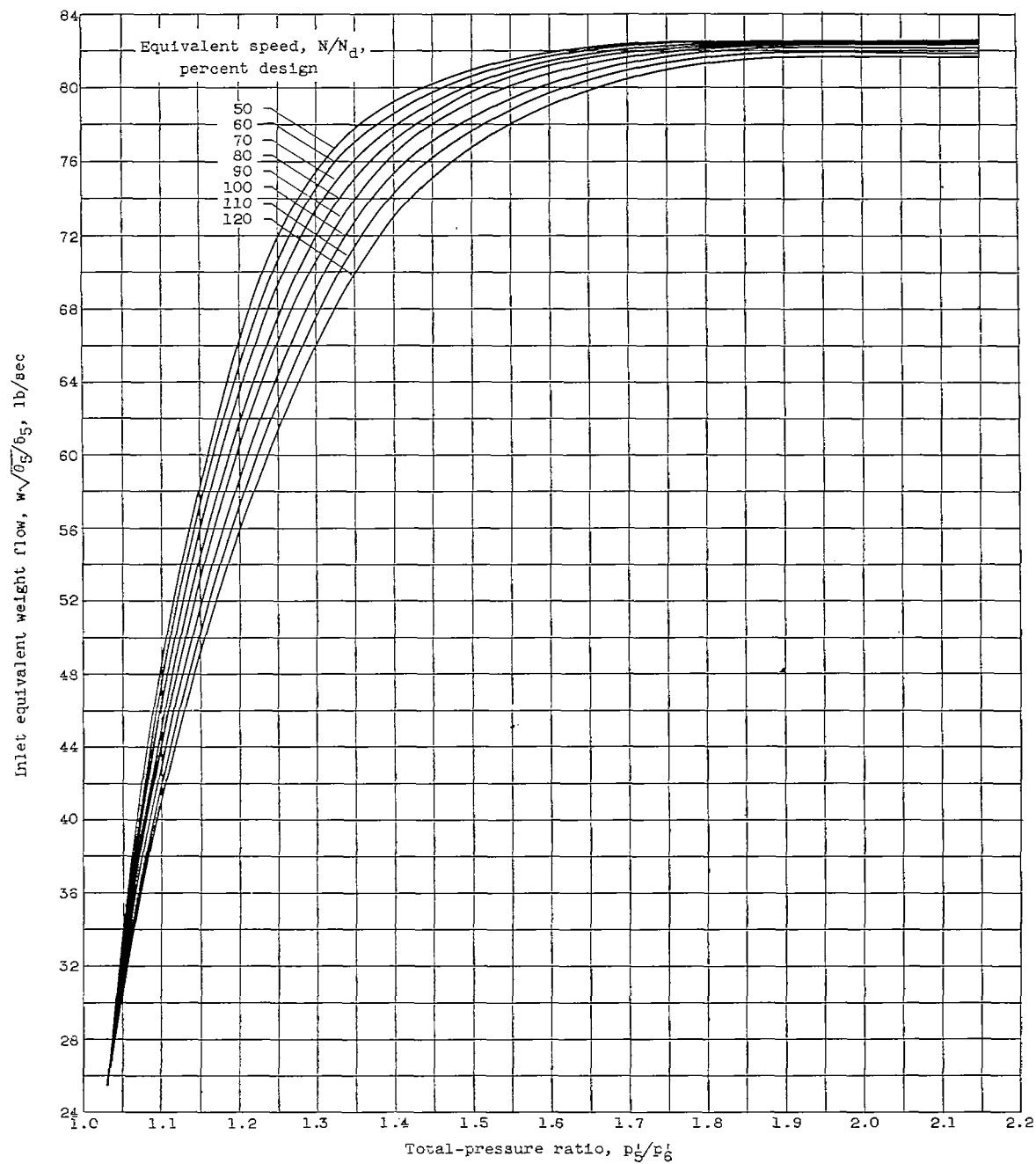
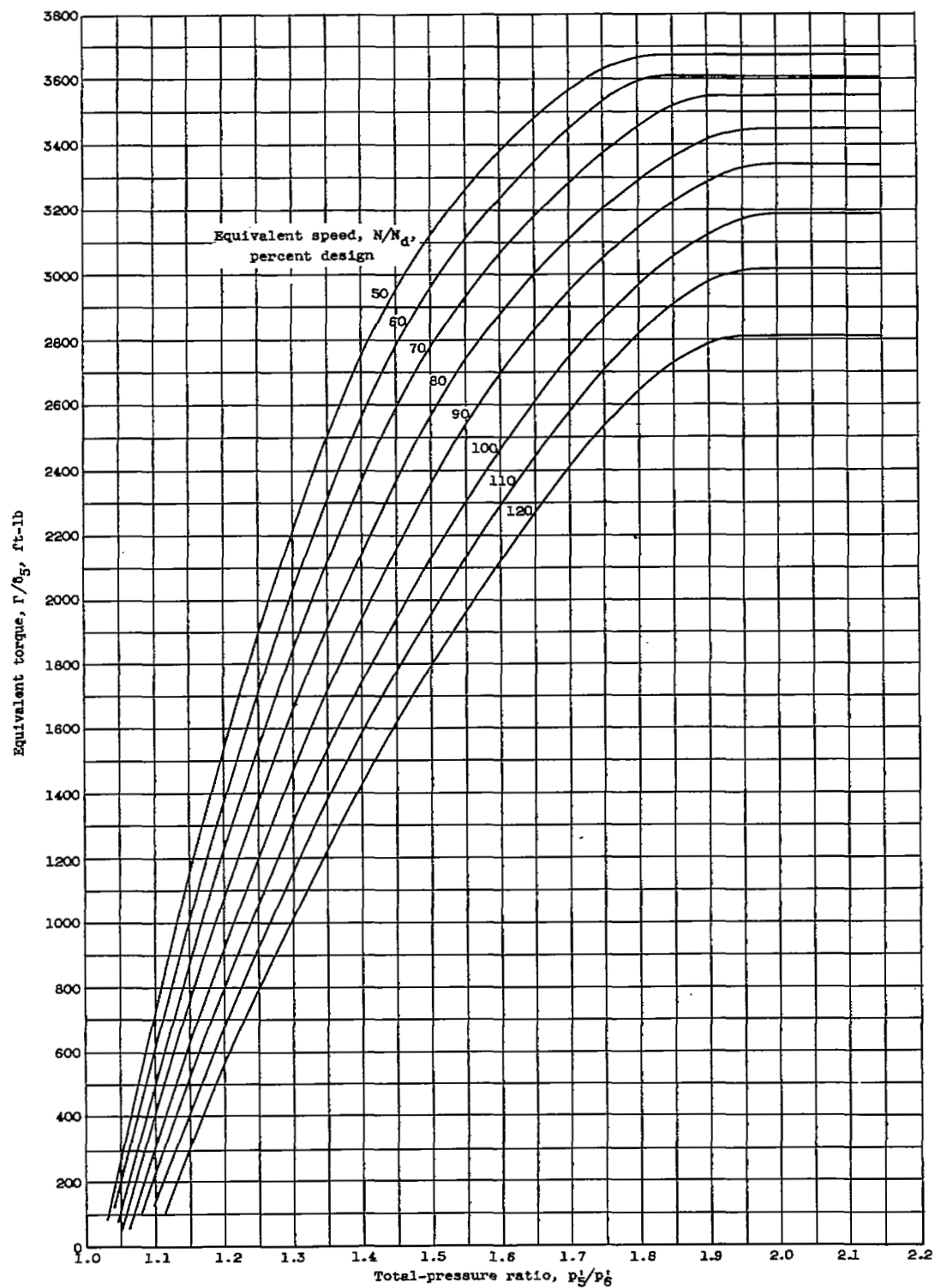


Figure 7. - Variation of turbine pressure ratio with percentage increase in turbine-inlet equivalent weight flow for compressor operation fixed at knee in surge line. Exhaust-nozzle area, 600 square inches.



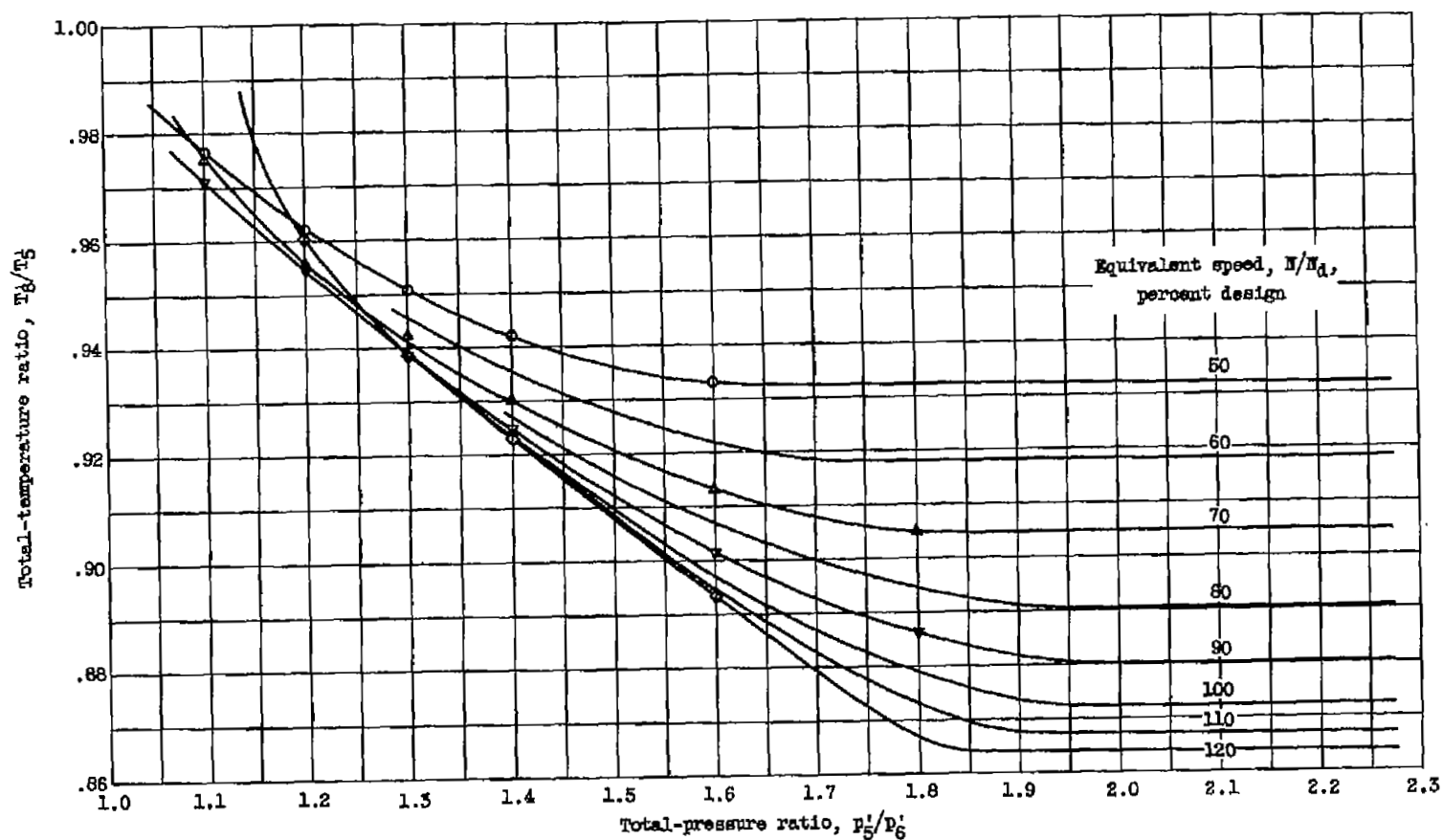
(a) Inlet equivalent weight flow.

Figure 8. - Third-stage performance with design stator setting.



(b) Equivalent torque.

Figure 8. - Continued. Third-stage performance with design stator setting.



(c) Temperature ratio.

Figure 8. - Concluded. Third-stage performance with design stator setting.

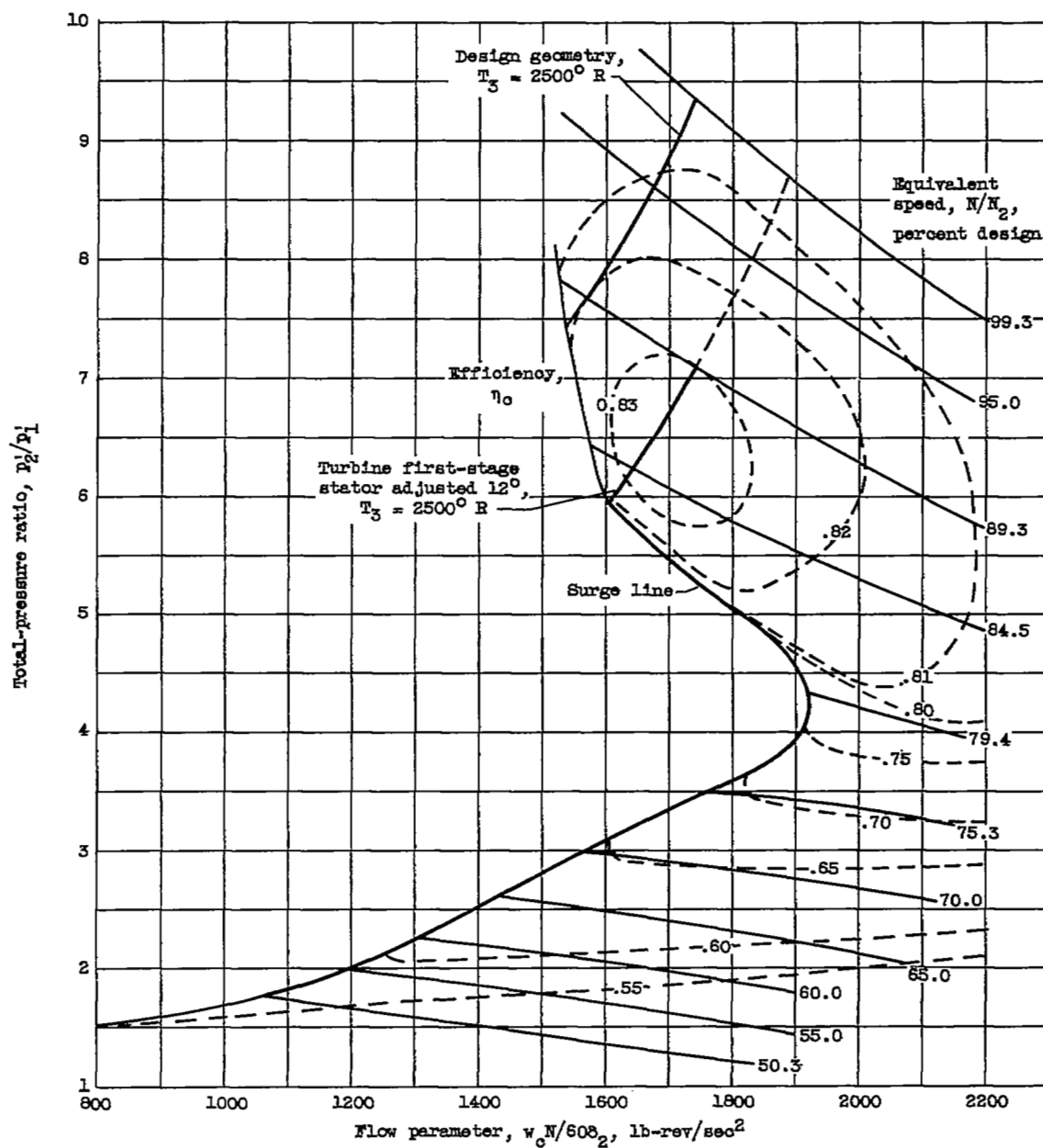
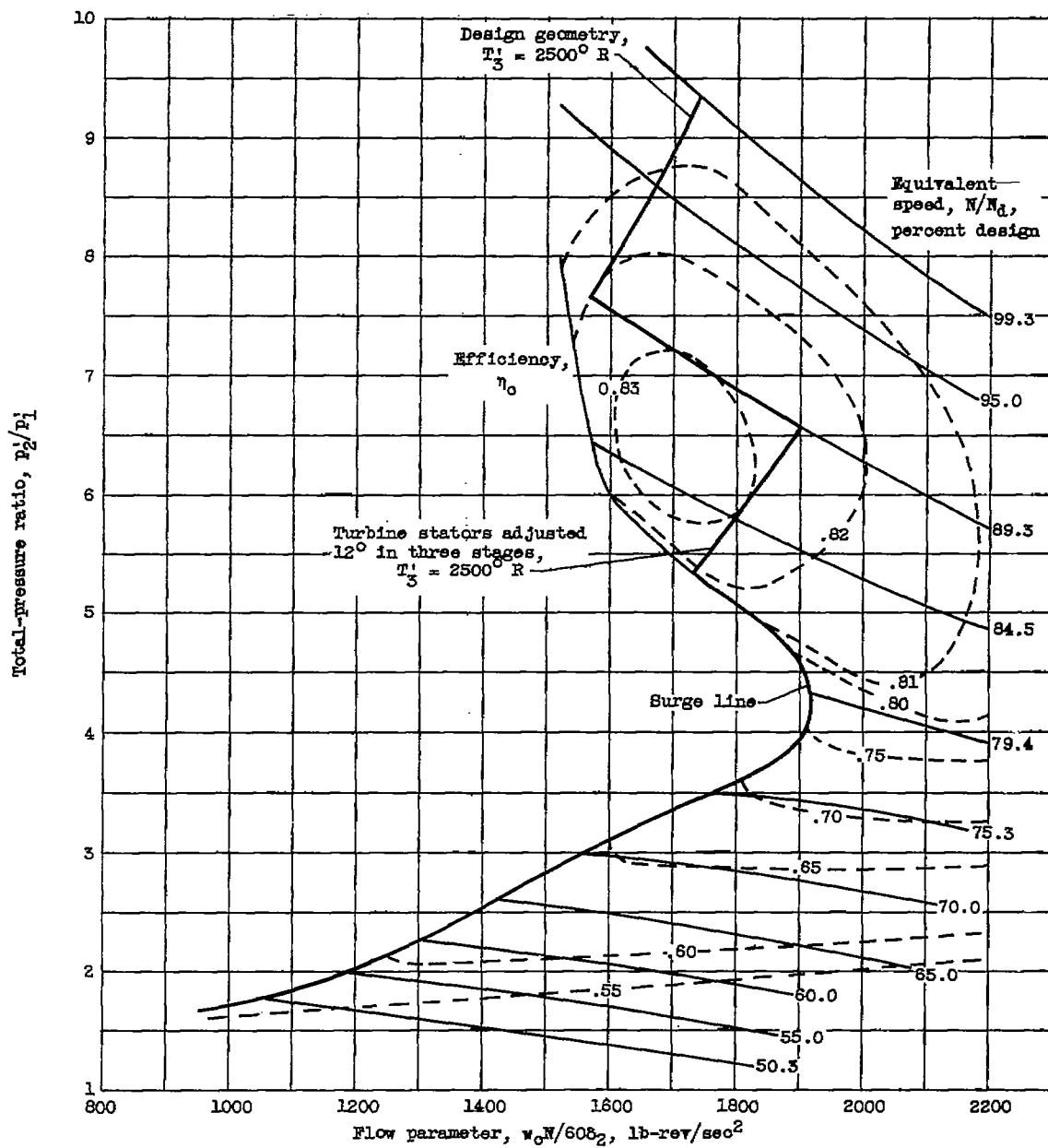
(a) Turbine first-stage stator adjustment,  $12^\circ$ .

Figure 9. - Compressor performance map and acceleration paths.





(b) Turbine stator adjustment in all three stages,  $12^\circ$ .

Figure 9. - Concluded. Compressor performance map and acceleration paths.

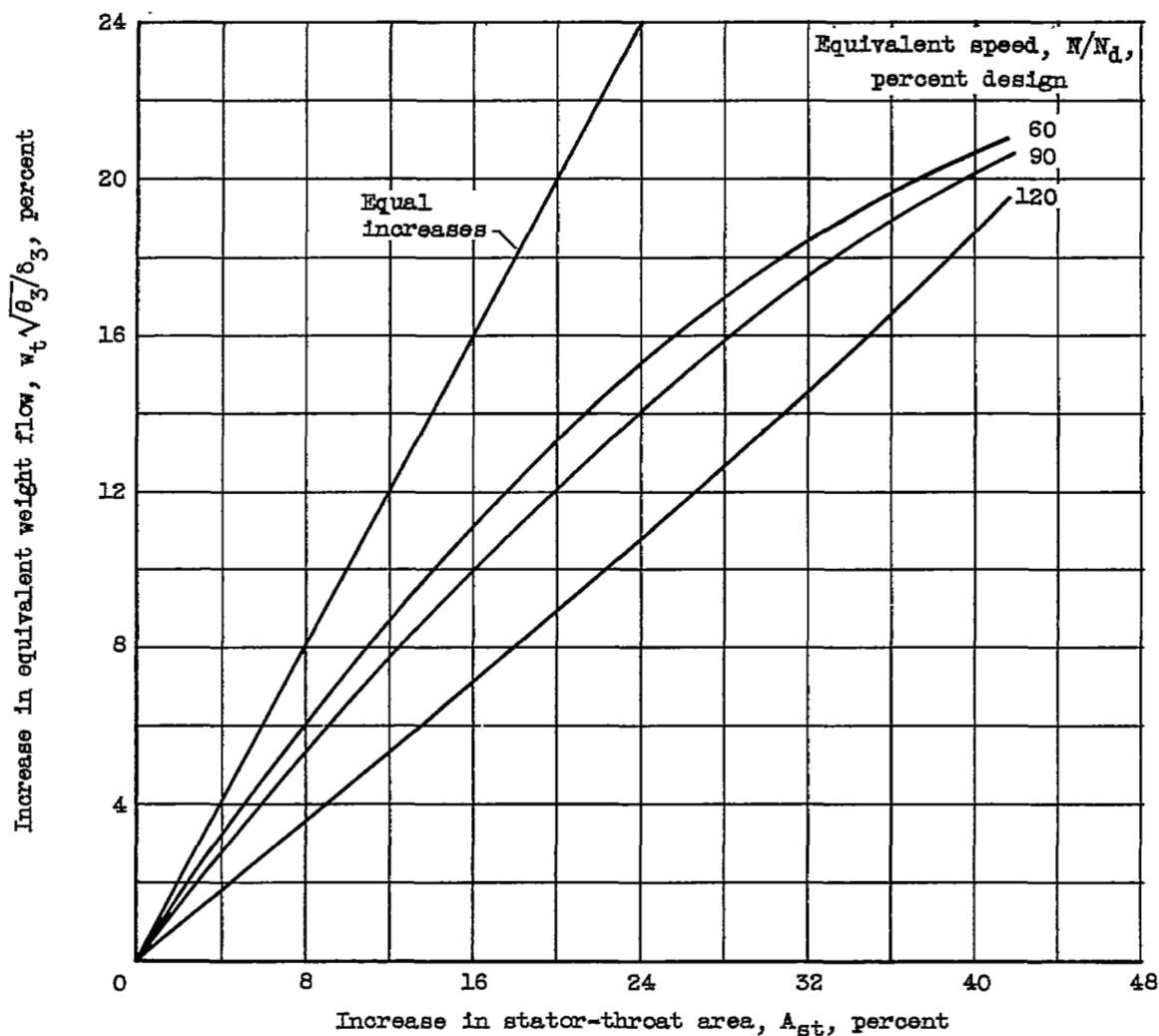
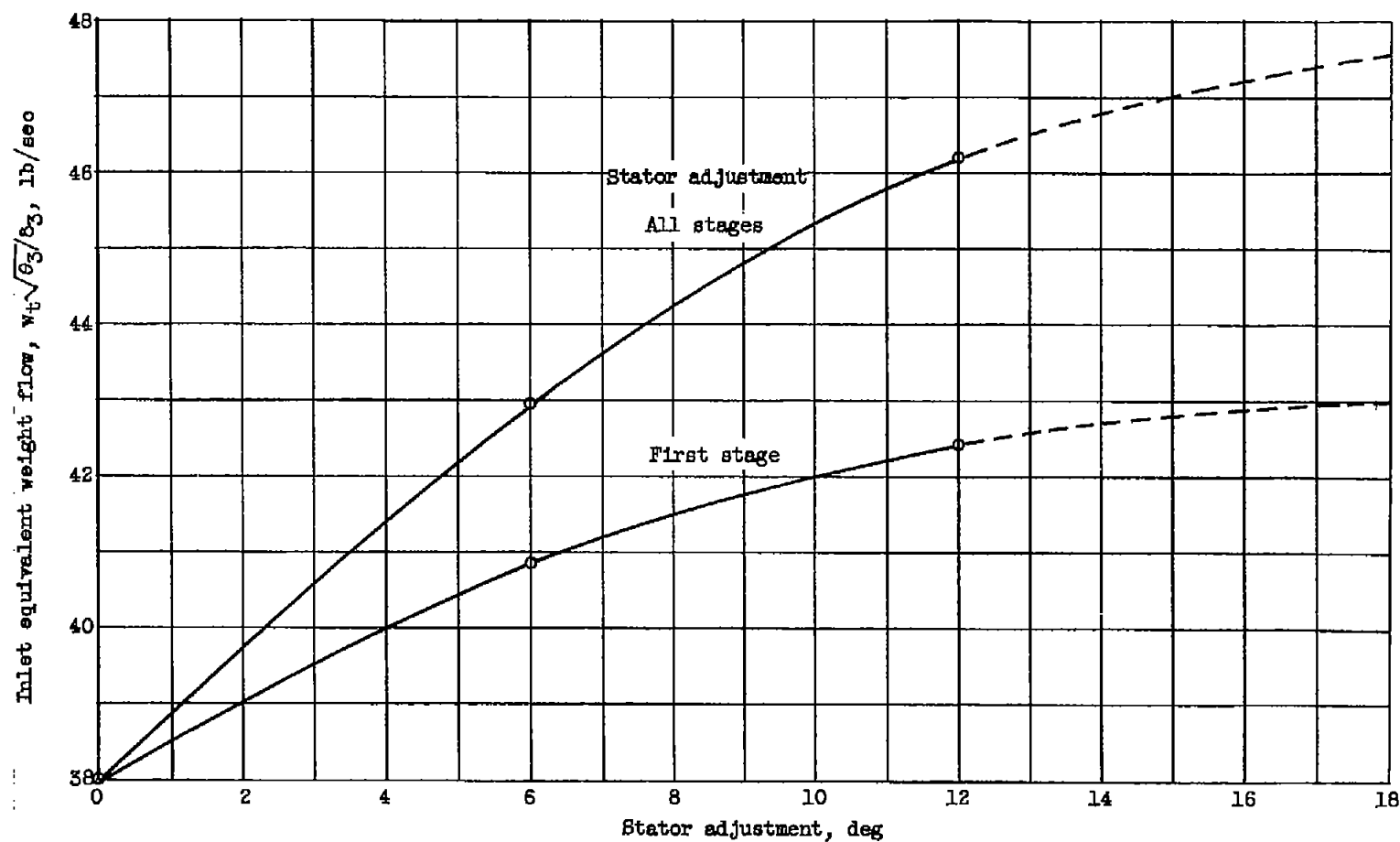
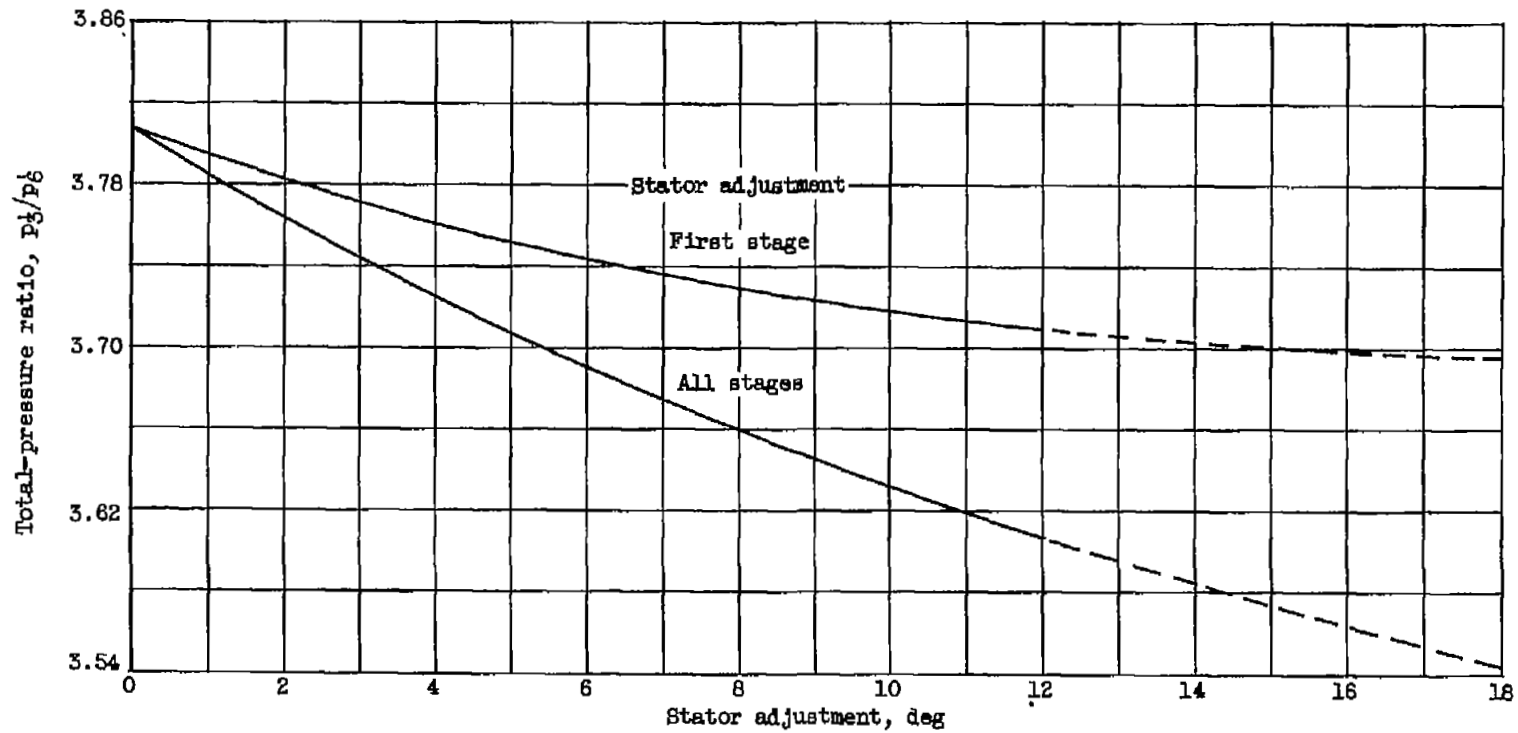


Figure 10. - Variation of increase in turbine first-stage inlet equivalent weight flow with increase in stator-throat area for three equivalent speeds. Turbine stage total-pressure ratio, 1.5.



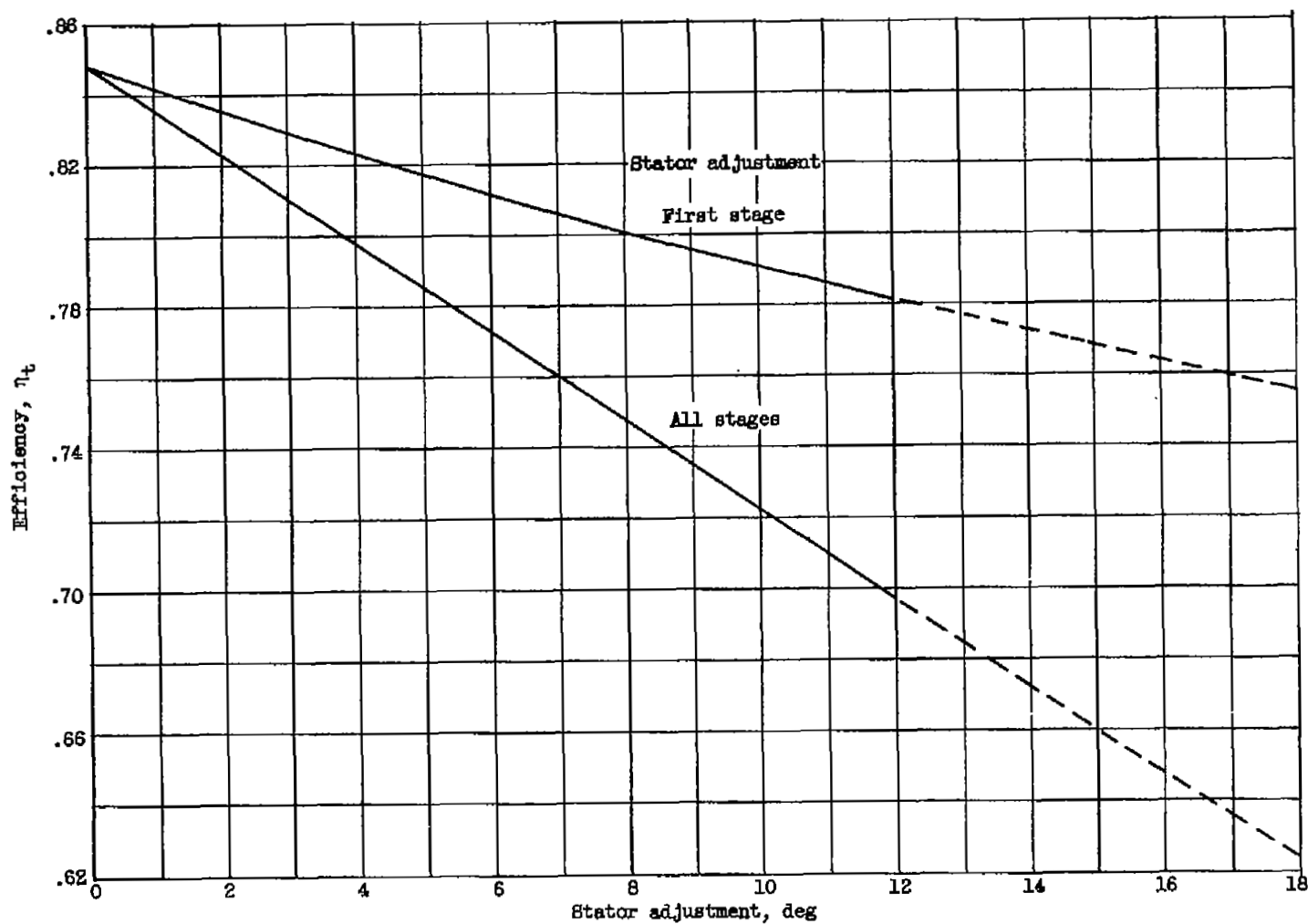
(a) Inlet equivalent weight flow.

Figure 11. - Variation of turbine parameters with stator adjustment for compressor operation at knee in surge line.



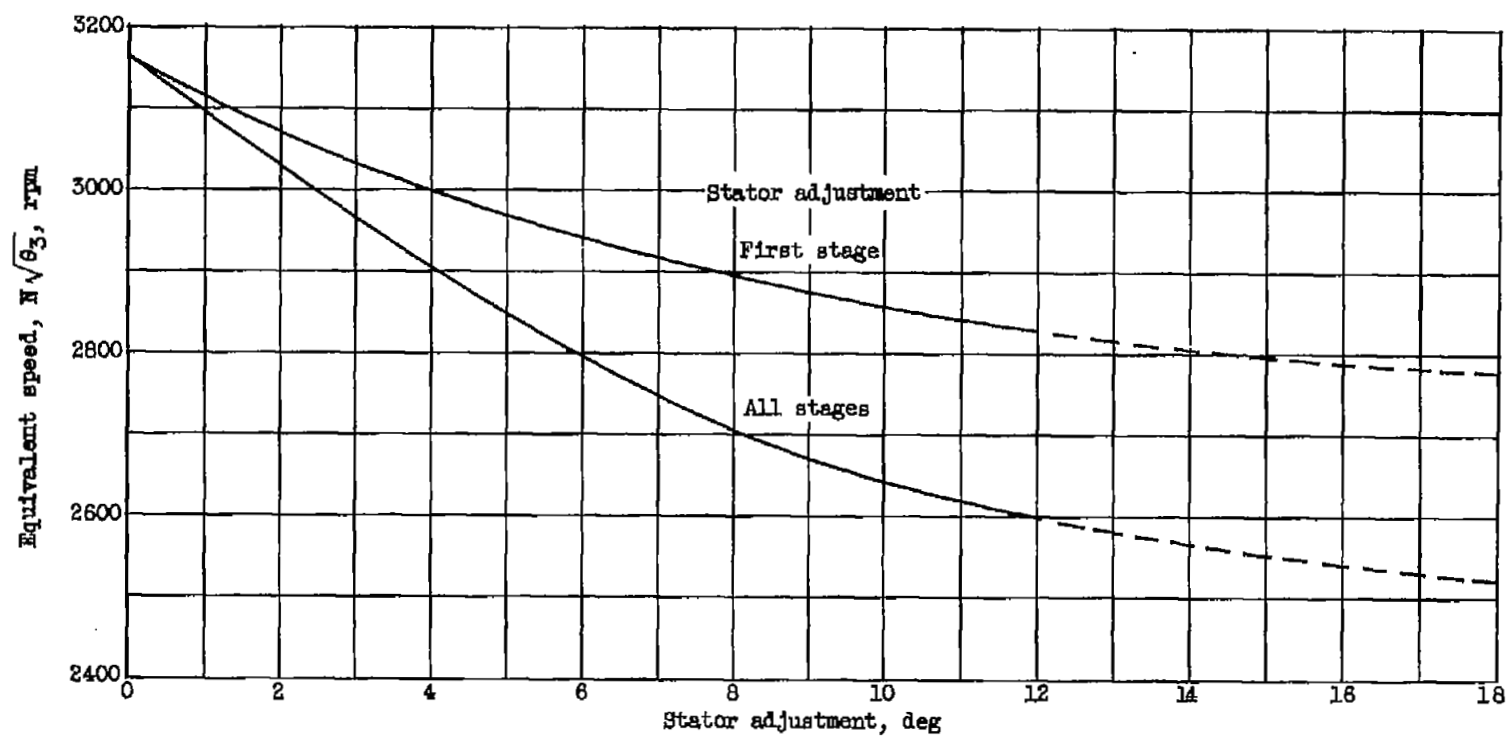
(b) Pressure ratio.

Figure 11. - Continued. Variation of turbine parameters with stator adjustment for compressor operation at knee in surge line.



(c) Efficiency.

Figure 11. - Continued. Variation of turbine parameters with stator adjustment for compressor operation at knee in surge line.



(d) Equivalent speed.

Figure 11. - Concluded. Variation of turbine parameters with stator adjustment for compressor operation at knee in surge line.

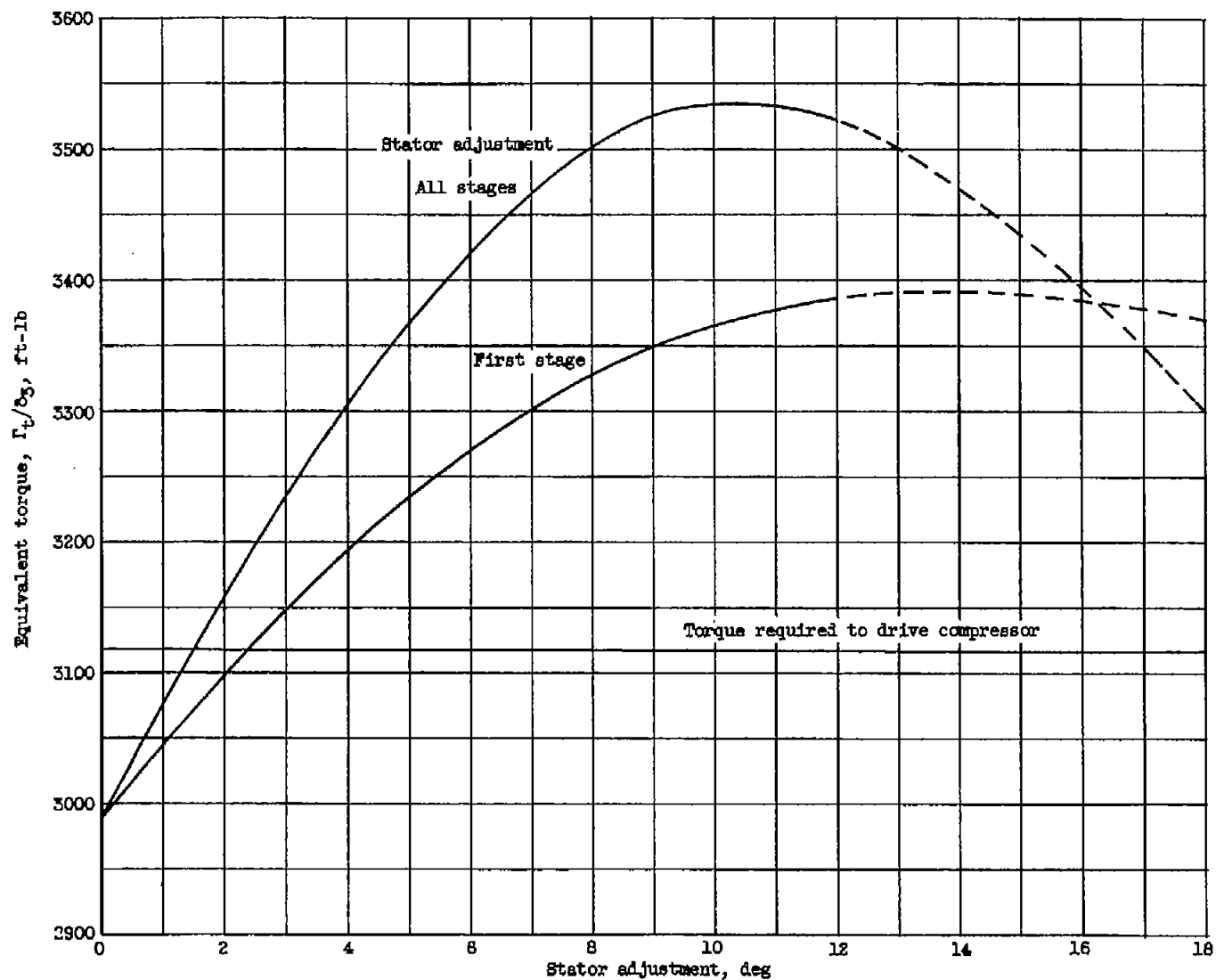
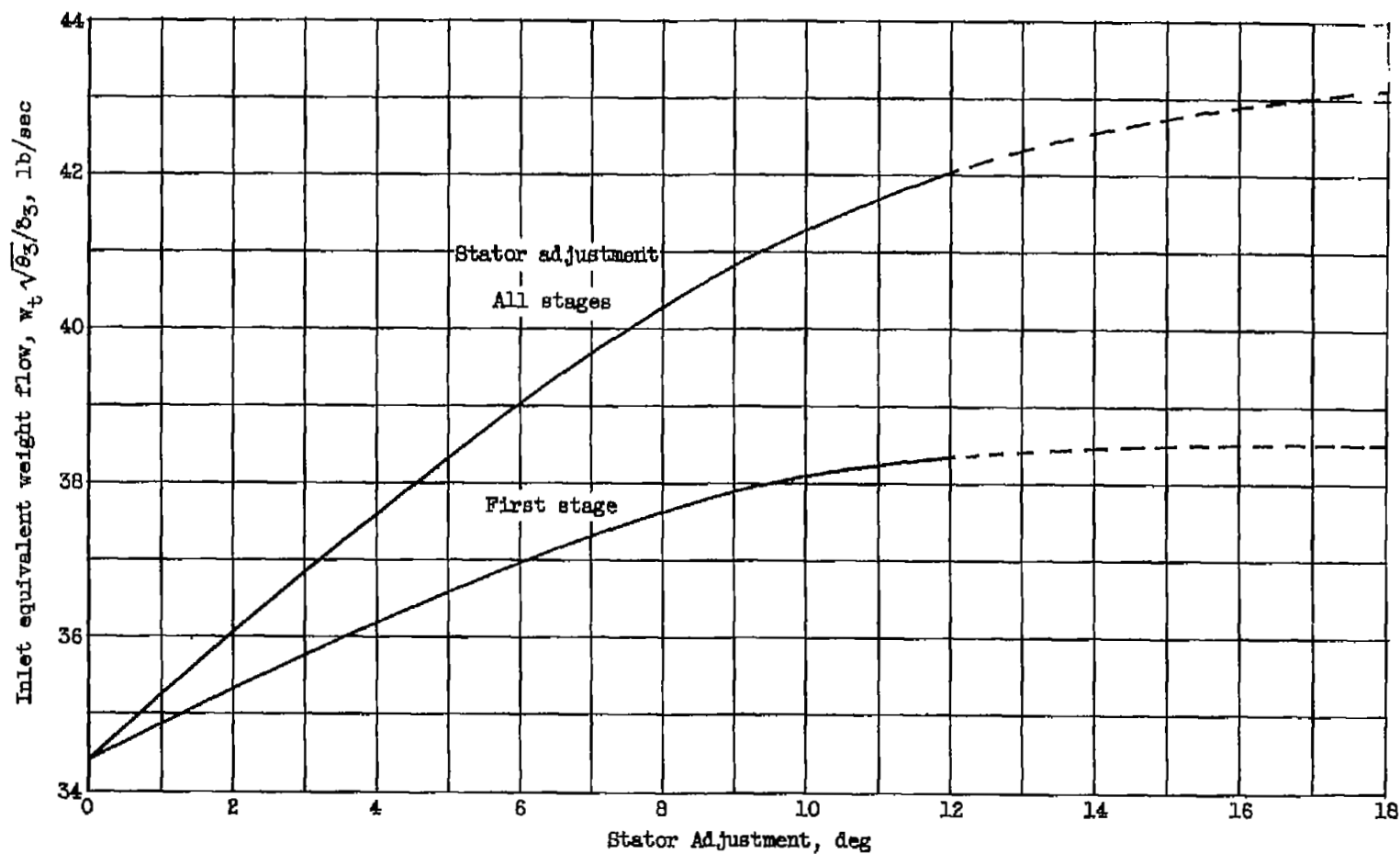


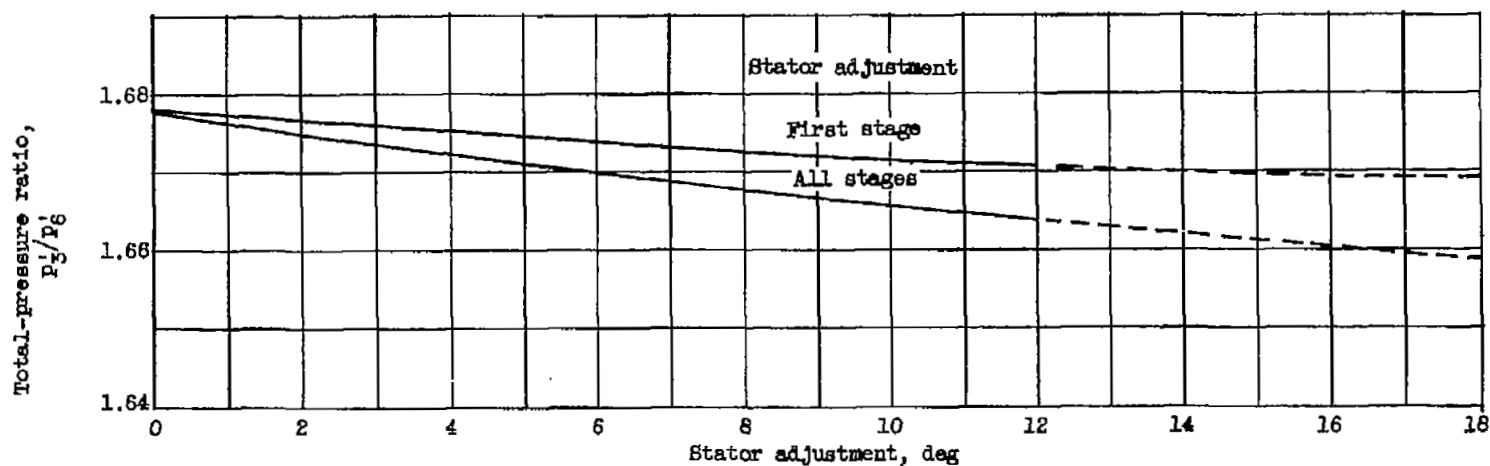
Figure 12. - Variation of turbine equivalent torque with stator adjustment for compressor operation at knee in surge line.



(a) Inlet equivalent weight flow.

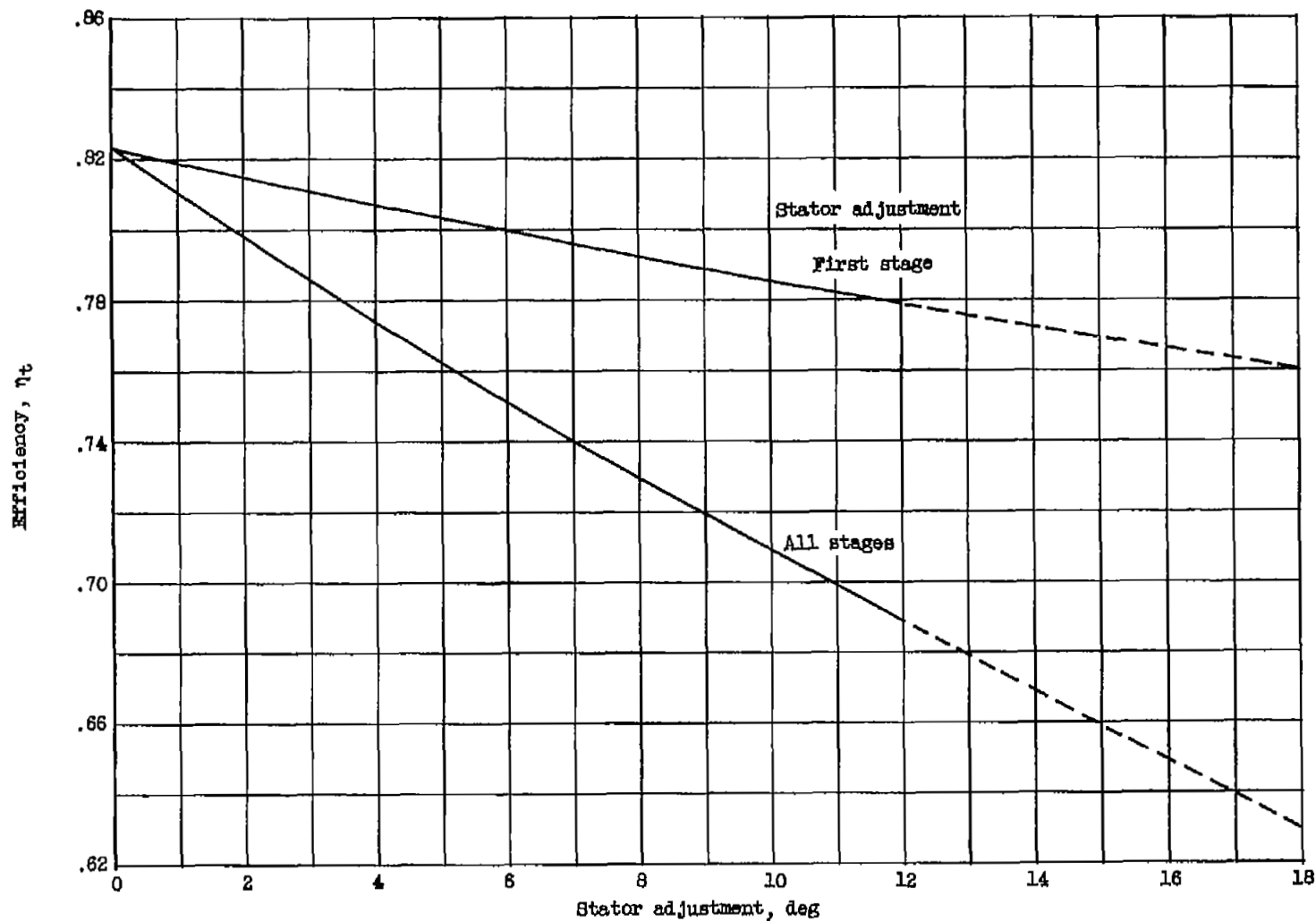
Figure 13. - Variation of turbine parameters with stator adjustment for compressor operation at idle speed and surge pressure ratio.





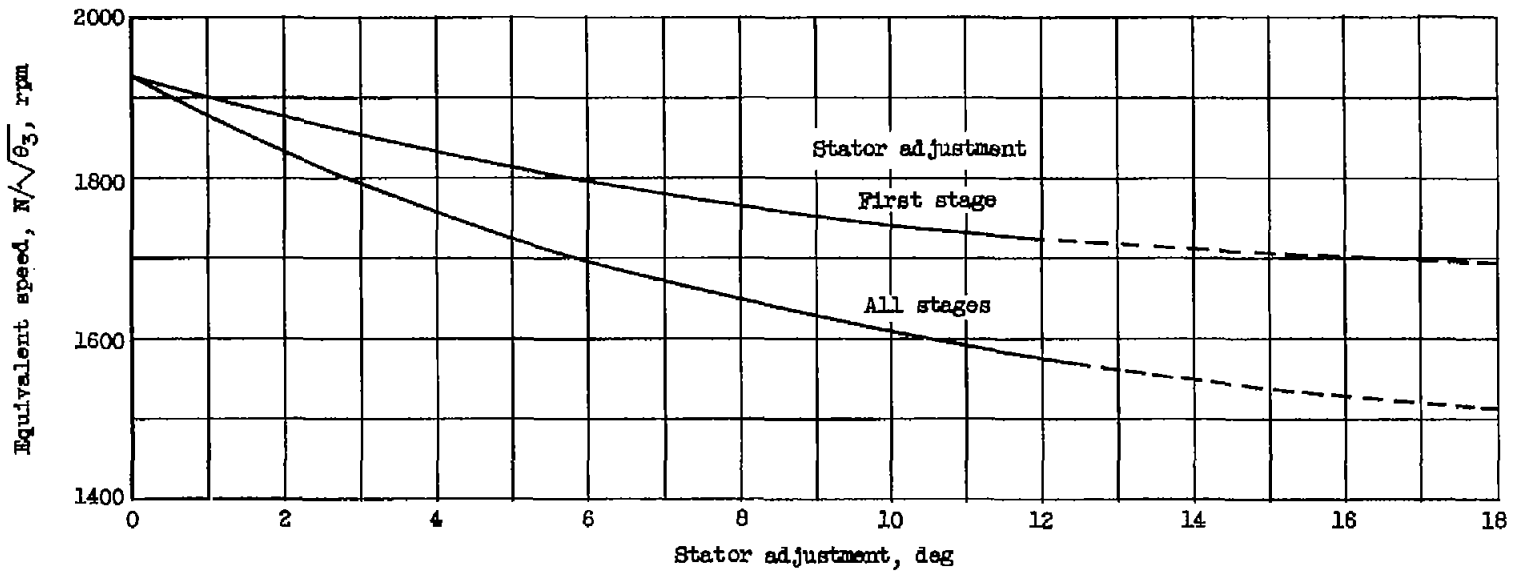
(b) Pressure ratio.

Figure 13. - Continued. Variation of turbine parameters with stator adjustment for compressor operation at idle speed and surge pressure ratio.



(c) Efficiency.

Figure 13. - Continued.. Variation of turbine parameters with stator adjustment for compressor operation at idle speed and surge pressure ratio.



(d) Equivalent speed.

Figure 13. - Concluded. Variation of turbine parameters with stator adjustment for compressor operation at idle speed and surge pressure ratio.

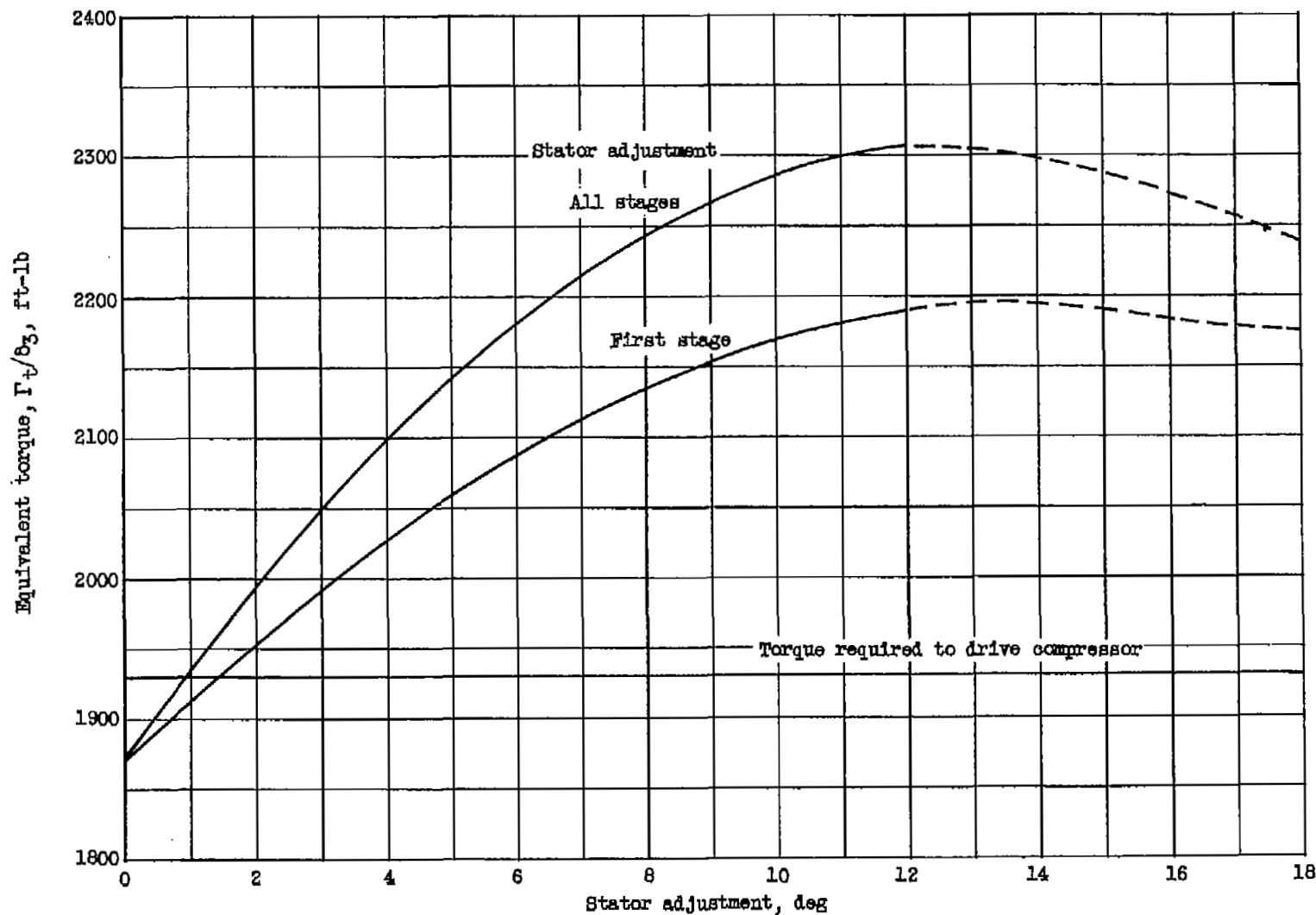
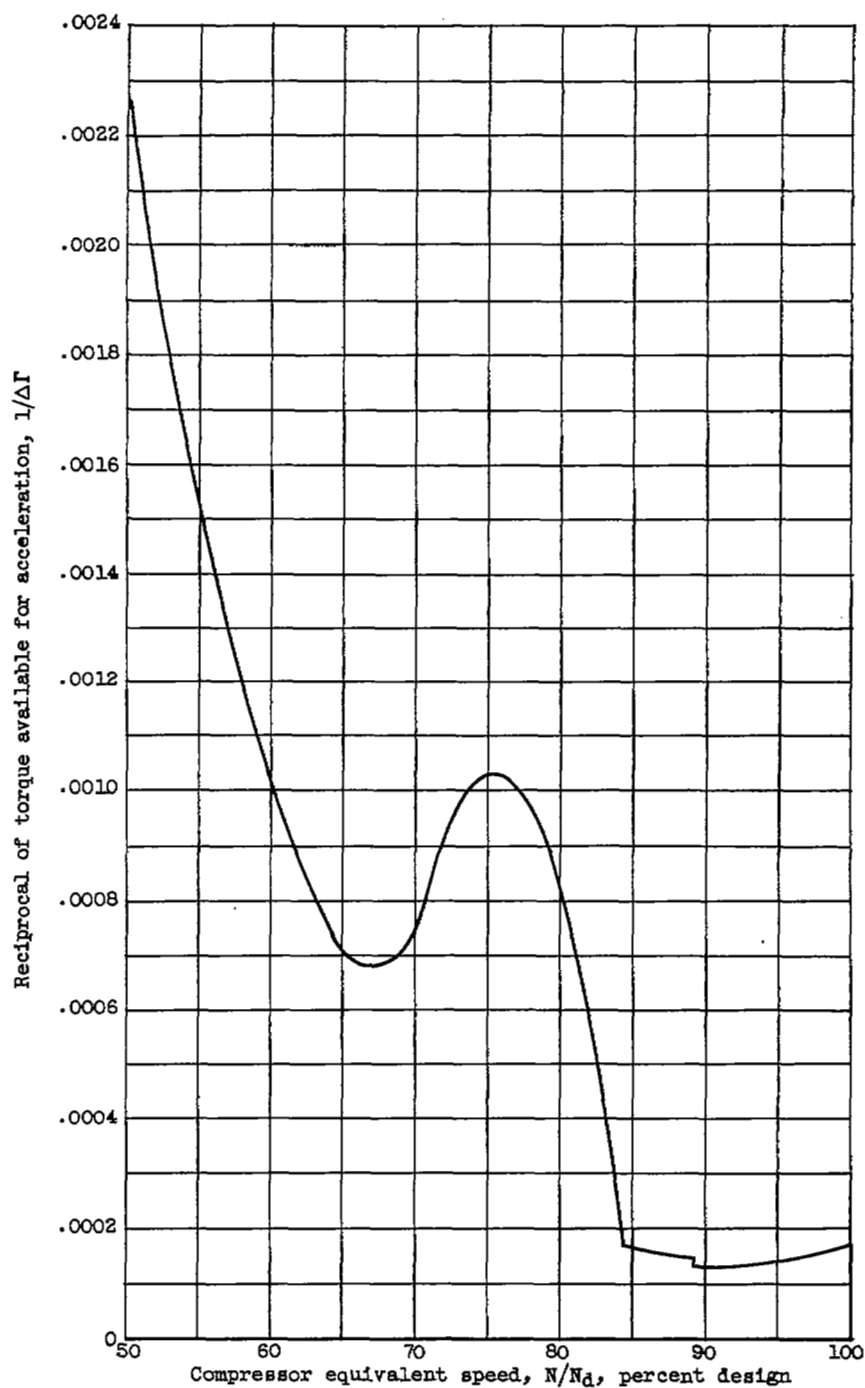
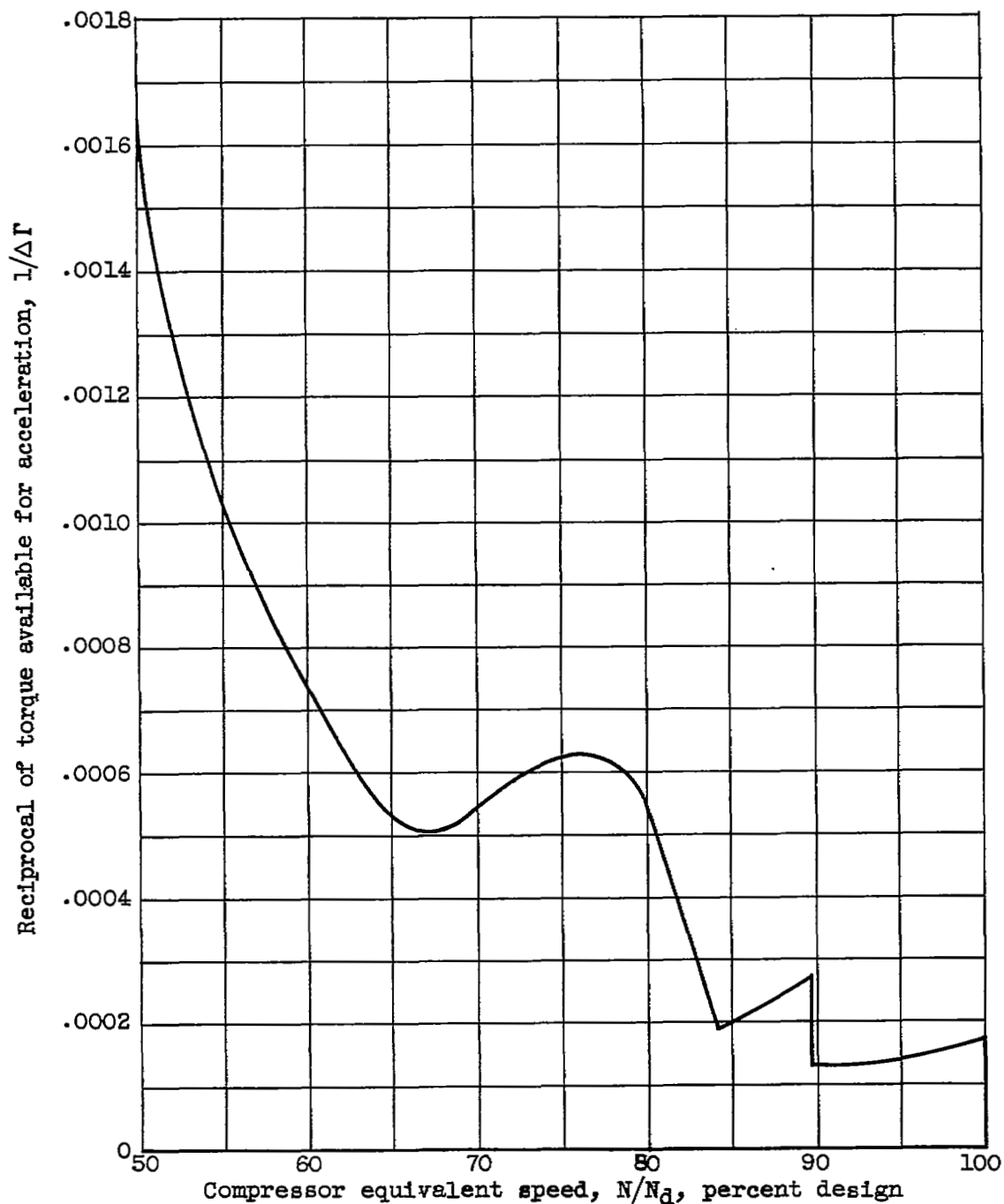


Figure 14. - Variation of turbine equivalent torque with stator adjustment for compressor operation at idle speed and surge pressure ratio.



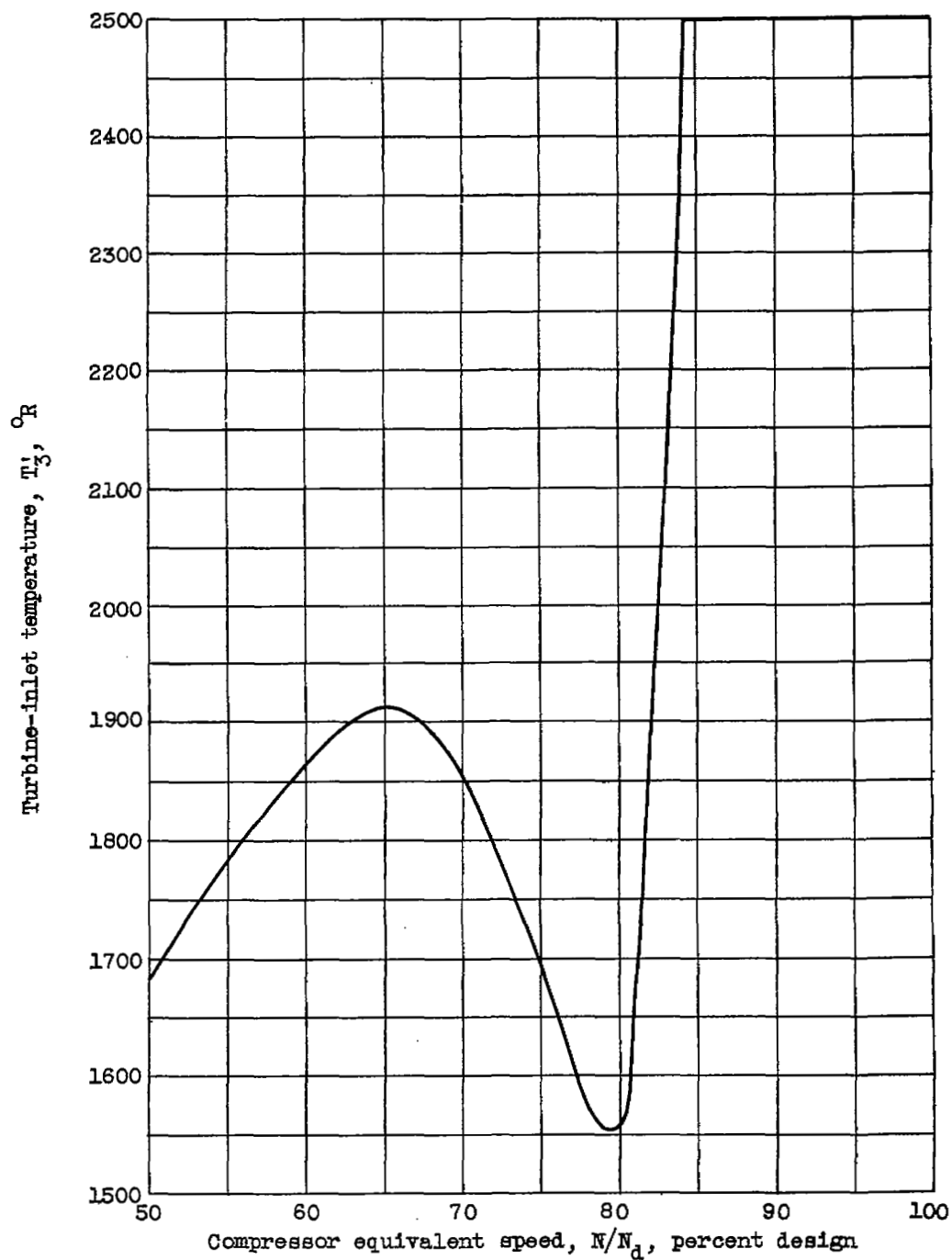
(a) First-stage stator adjustment,  $12^\circ$ . Total acceleration time, 9.6 seconds.

Figure 15. - Graphical integration for acceleration at surge pressure ratio; maximum turbine-inlet temperature,  $2500^\circ \text{R}$ .



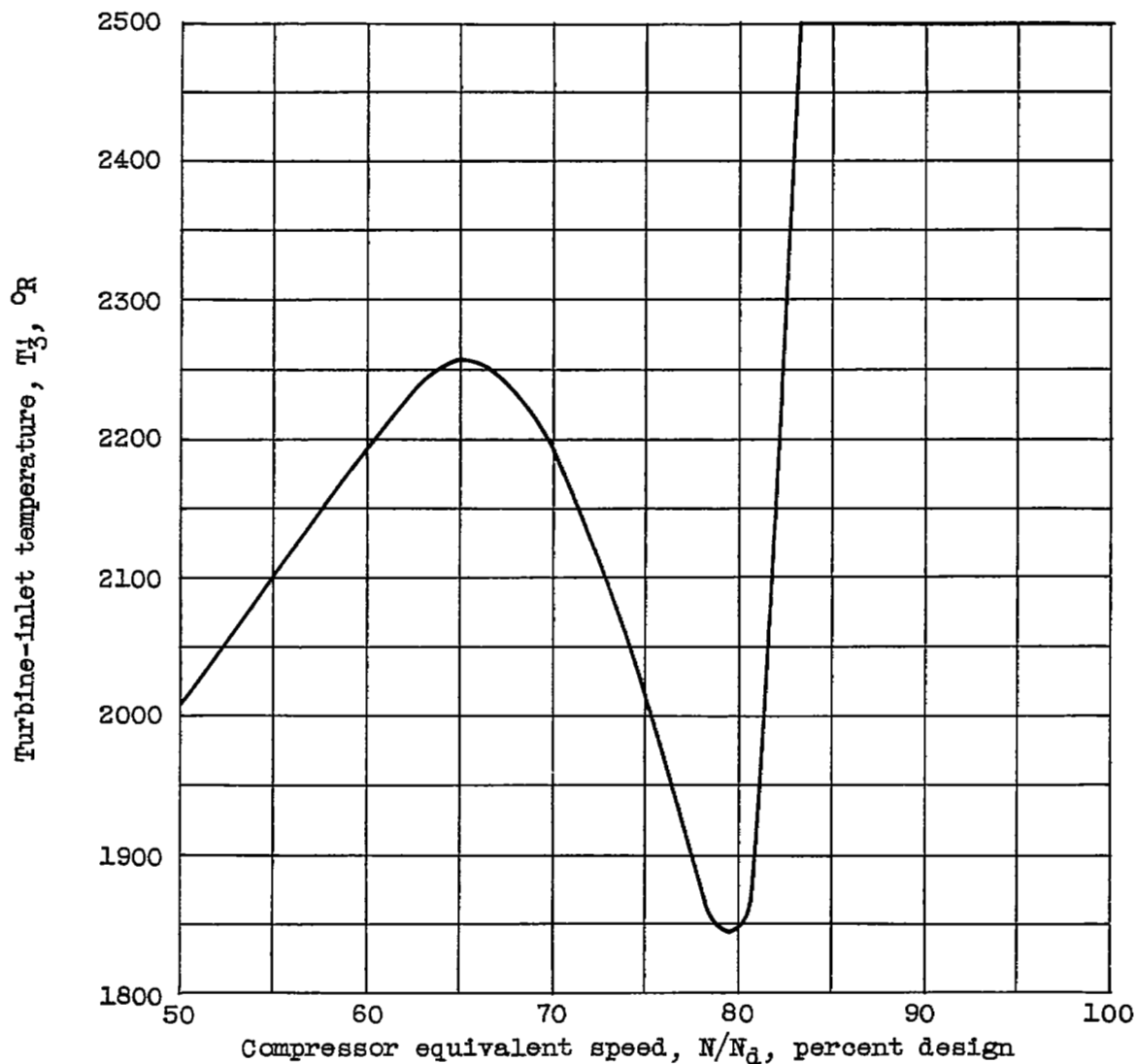
(b) Stator adjustment in all three stages,  $12^\circ$ . Total acceleration time, 7.0 seconds.

Figure 15. - Concluded. Graphical integration for acceleration at surge pressure ratio; maximum turbine-inlet temperature,  $2500^\circ\text{R}$ .



(a) First-stage stator adjustment,  $12^\circ$ .

Figure 16. - Variation of turbine-inlet temperature with speed at surge pressure ratio; maximum turbine-inlet temperature,  $2500^\circ\text{R}$ .



(b) Stator adjustment in all three stages,  $12^\circ$ .

Figure 16. - Concluded. Variation of turbine-inlet temperature with speed at surge pressure ratio; maximum turbine-inlet temperature,  $2500^\circ$  R.



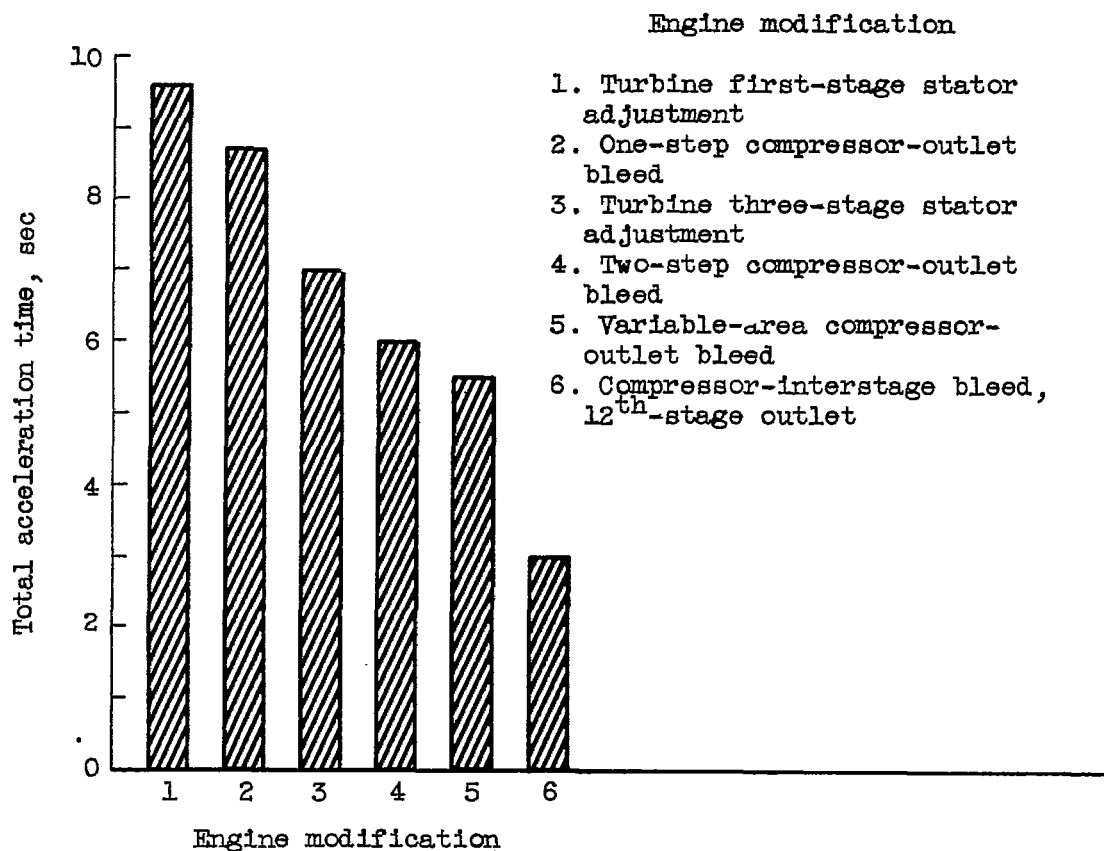


Figure 17. - Comparison of acceleration times for several engine modifications. Compressor operation along surge line; maximum turbine-inlet temperature, 2500° R; exhaust-nozzle area, 600 square inches.

NASA Technical Library



3 1176 01435 4121

